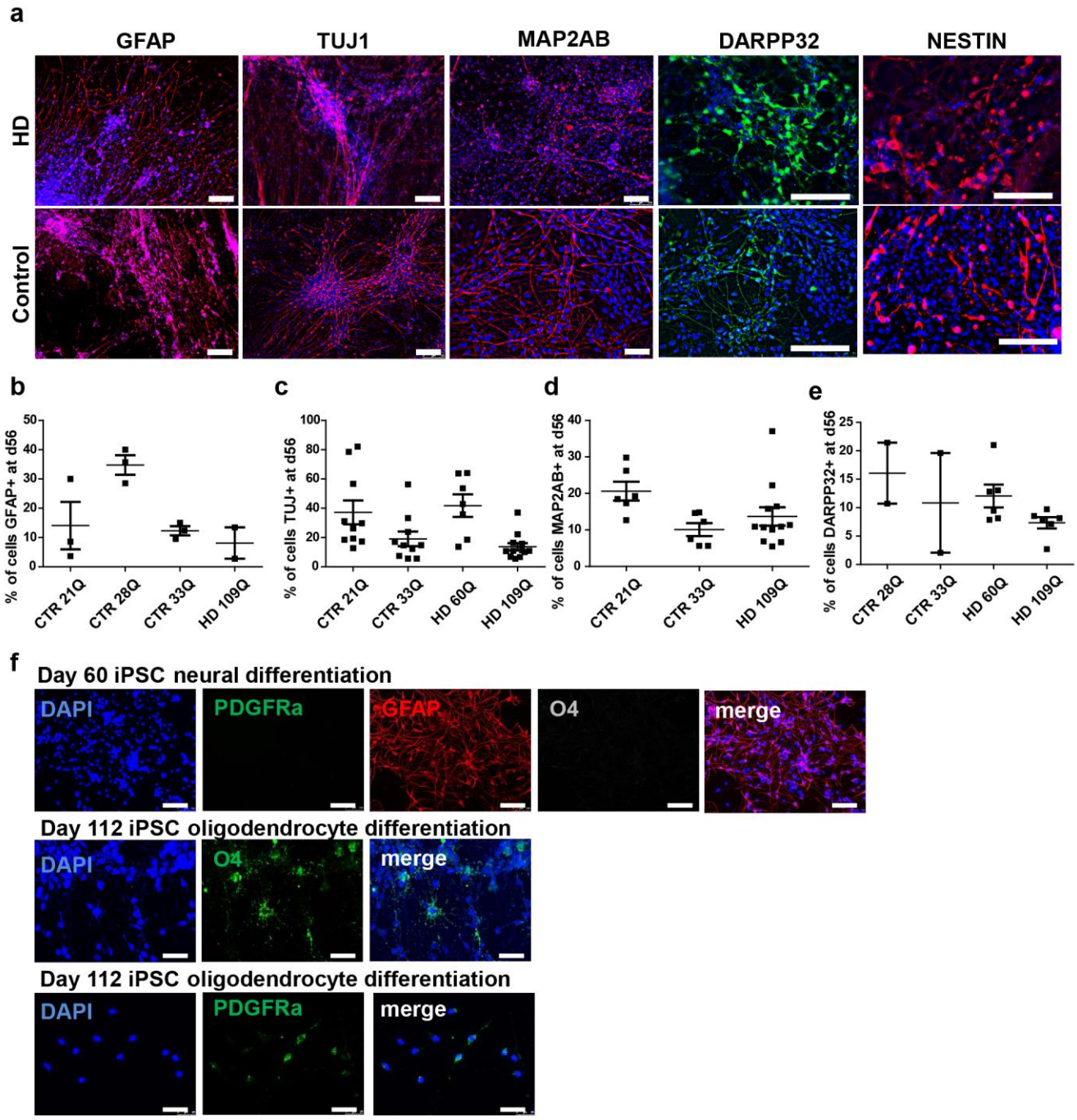

Supplementary Figure 1

Staining and quantification of neuronal and oligodendrocyte differentiation markers.

(a) Representative images of immunocytochemistry at day 56 of differentiation demonstrate that both HD (HD109 pictured here) and non-disease (CTR21 pictured here) iPSC lines can generate glial (GFAP) and neuronal (TUJ1, MAP2ab, DARPP32) cells. Scale bar represents 100 mm. (b) Non-biased stereological counts of TUJ1 at day 56 of differentiation indicate that there is no difference in the percent of cells TUJ1-positive between HD and non-disease (CTR). The HD109Q line did have significantly lower TUJ1-positive cells than the CTR21Q and the HD60Q lines (one-way ANOVA, * $p<0.05$, ** $p<0.01$); however, this reflects line-to-line variability versus a CAG repeat effect. (c) Non-biased stereological counts of MAP2ab at day 56 of differentiation indicate that there is no difference in the percent of cells MAP2ab-positive between HD and non-diseased. (d) Non-biased stereological counts of DARPP32 at day 56 of differentiation indicate that while there is no difference in the percent of DARPP32-positive cells between HD and non-disease. (e) Non-

biased stereological counts of GFAP indicate there is no difference in the percent of cells GFAP-positive between HD and non-diseased. (f) Glial markers PDGFRα and O4 were found to be absent in the iPSC-neural cultures at day 60 of differentiation, whereas at day 112 of oligodendrocyte differentiation from iPSCs, these glial markers were found. Approximately 1000 cells were counted per slide for three independent differentiations.

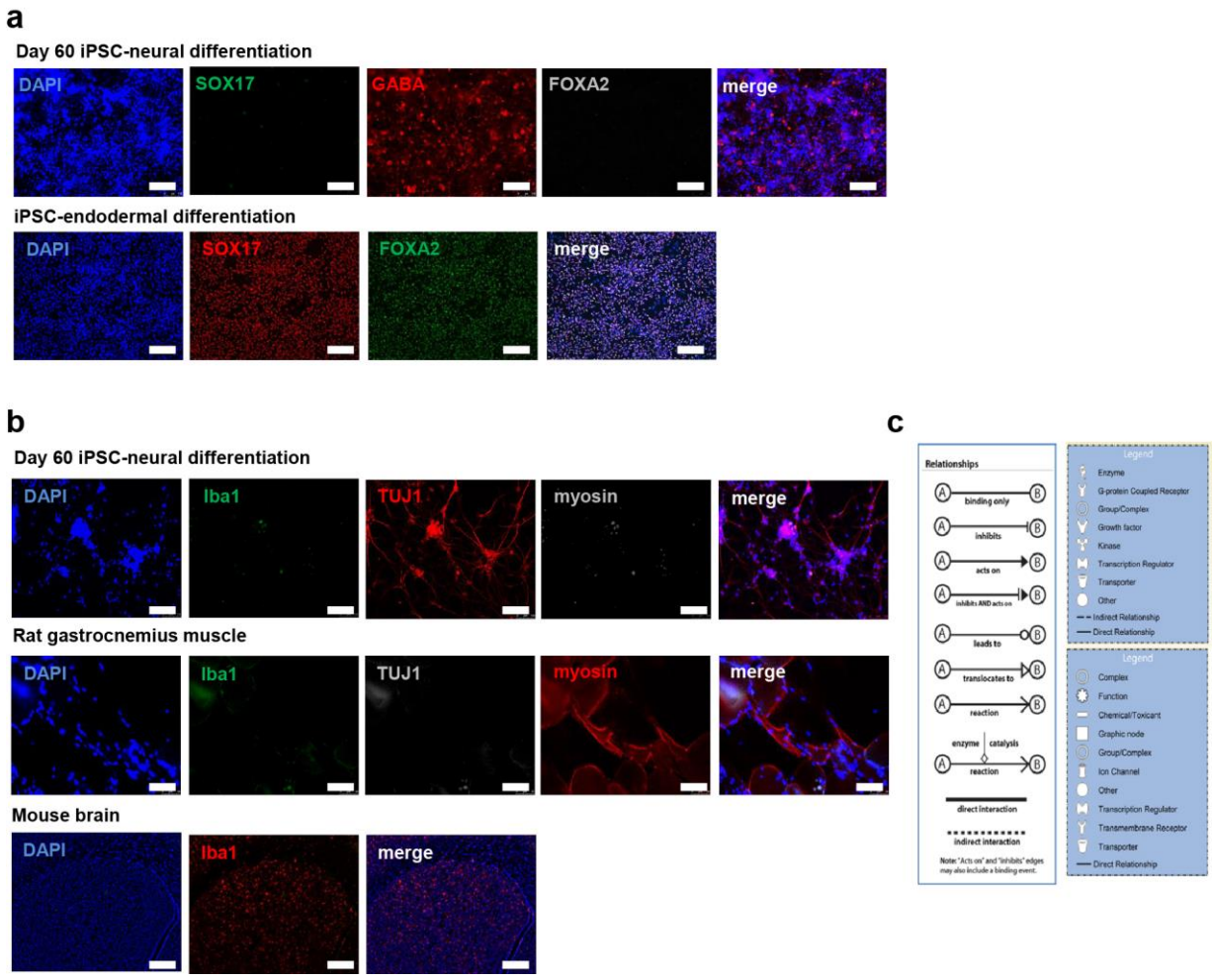

Supplementary Figure 2

Staining of endoderm, mesoderm and microglial differentiation markers and legend for IPA results.

(a) The endodermal markers SOX17 and FOXA2 were absent in the iPSC-neural cultures (CTR21) at day 60 of differentiation, but they were present in differentiated cultures of iPSC-endoderm (CTR33). (b) The microglial marker Iba1 was absent in day 60 iPSC-neural cultures, but present in wild-type mouse brain sections. Likewise, the mesodermal marker myosin was absent in day 60 iPSC-neural cultures, but present in sections of rat gastrocnemius muscle. (c) IPA gene symbols and relationships. IPA legend for gene networks and relationships/edges.

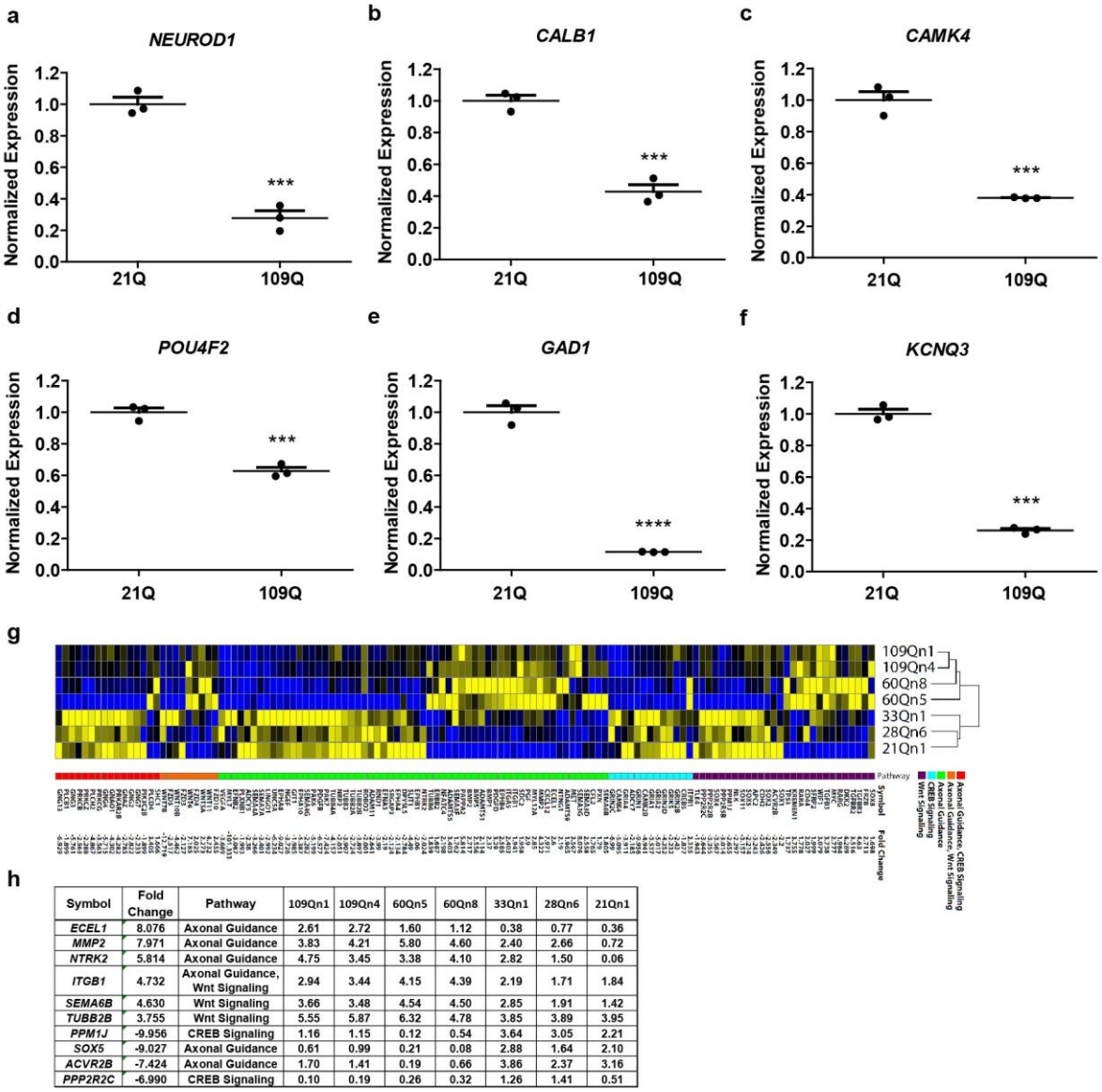

h

Symbol	Fold Change	Pathway	109Qn1	109Qn4	60Qn5	60Qn8	33Qn1	28Qn6	21Qn1
ECEL1	8.076	Axonal Guidance	2.61	2.72	1.60	1.12	0.38	0.77	0.36
MMP2	7.971	Axonal Guidance	3.83	4.21	5.80	4.60	2.40	2.66	0.72
NTRK2	5.814	Axonal Guidance	4.75	3.45	3.38	4.10	2.82	1.50	0.06
ITGB1	4.732	Axonal Guidance, Wnt Signaling	2.94	3.44	4.15	4.39	2.19	1.71	1.84
SEMA6B	4.630	Wnt Signaling	3.66	3.48	4.54	4.50	2.85	1.91	1.42
TUBB2B	3.755	Wnt Signaling	5.55	5.87	6.32	4.78	3.85	3.89	3.95
PPM1J	-9.956	CREB Signaling	1.16	1.15	0.12	0.54	3.64	3.05	2.21
SOX5	-9.027	Axonal Guidance	0.61	0.99	0.21	0.08	2.88	1.64	2.10
ACVR2B	-7.424	Axonal Guidance	1.70	1.41	0.19	0.66	3.86	2.37	3.16
PPP2R2C	-6.990	CREB Signaling	0.10	0.19	0.26	0.32	1.26	1.41	0.51

Supplementary Figure 3

Quantitative PCR supports altered gene expression identified by RNA-seq and hierarchical clustering of genes differentially expressed in several top canonical pathways.

(a-f) New differentiations of representative non-disease (21Q) and HD (109Q) lines were performed and select genes evaluated by RT-qPCR. All exhibited altered expression consistent with that identified by RNA-seq. Two differentiated wells of each line were pooled for RNA extraction and three technical replicates of qPCR performed. A statistical difference in gene expression was determined using an unpaired two-tailed t-test in GraphPad Prism. *NEUROD1*: P=0.0003, t=11.38, df=4; *CALB1*: P=0.0005, t=10.23, df=4; *CAMK4*: P=0.0003, t=11.72, df=4; *POU4F2*: P=0.0005, t=10.25, df=4; *GAD1*: P<0.0001, t=21.15; df=4; *KCNQ3*: P<0.0001, t=24.22, df=4). (g) Heat map showing hierarchical clustering of log2 transformed gene expression values (RPKMs) of the significantly differentially expressed genes (1869) found in several of the top affected canonical pathways (colors displayed by row min and max values, yellow = higher and blue = lower expression). Genes/rows are sorted by involvement in specific pathways that have been marked by color and shows pathway convergence on key regulator genes founds in both axonal guidance and either CREB or WNT signaling. Fold change is shown to the right of the gene symbol and represents the average change of HD/non-disease. A clear pattern of differential gene expression in each pathway provides an indication of activation or inhibition of the pathway. (h) Table showing normalized log2 gene expression values of the top up and down regulated genes in Fig. S3g. Each gene is categorized by pathway involved and HD vs non-disease fold change is displayed.

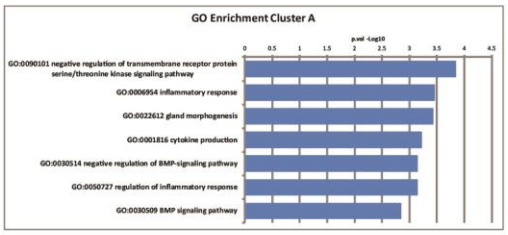
GO Enrichment Cluster A
p.val -Log10
0 0.5 1 1.5 2 2.5 3 3.5 4 4.5
GO:0090101 negative regulation of transmembrane receptor protein serine/threonine kinase signaling pathway
GO:0006954 inflammatory response
GO:0022612 gland morphogenesis
GO:0001816 cytokine production
GO:0030514 negative regulation of BMP signaling pathway
GO:0050727 regulation of inflammatory response
GO:0030509 BMP signaling pathway

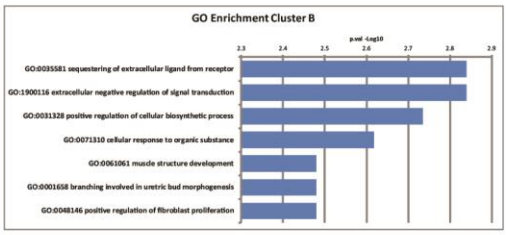
GO Enrichment Cluster B
p.val -Log10
2.3 2.4 2.5 2.6 2.7 2.8 2.9
GO:0035581 sequestering of extracellular ligand from receptor
GO:1900116 extracellular negative regulation of signal transduction
GO:0031328 positive regulation of cellular biosynthetic process
GO:0071310 cellular response to organic substance
GO:0061061 muscle structure development
GO:0001658 branching involved in ureteric bud morphogenesis
GO:0048146 positive regulation of fibroblast proliferation

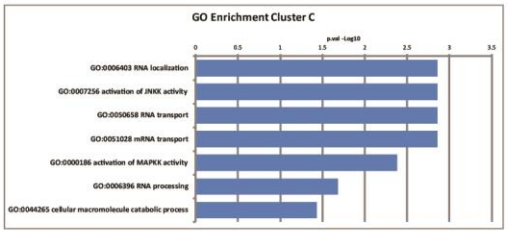
GO Enrichment Cluster C
p.val -Log10
0 0.5 1 1.5 2 2.5 3 3.5
GO:0006403 RNA localization
GO:0007256 activation of JNKK activity
GO:0050658 RNA transport
GO:0051028 mRNA transport
GO:0000186 activation of MAPKK activity
GO:0006396 RNA processing
GO:0044265 cellular macromolecule catabolic process

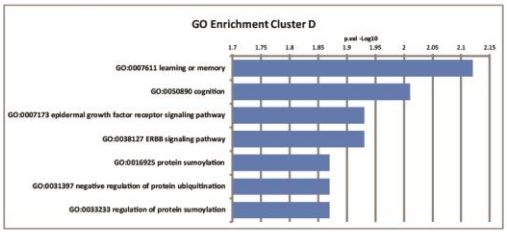
GO Enrichment Cluster D
p.val -Log10
1.7 1.75 1.8 1.85 1.9 1.95 2 2.05 2.1 2.15
GO:0007611 learning or memory
GO:0050890 cognition
GO:0007173 epidermal growth factor receptor signaling pathway
GO:0038127 ERBB signaling pathway
GO:0016925 protein sumoylation
GO:0031397 negative regulation of protein ubiquitination
GO:0033233 regulation of protein sumoylation

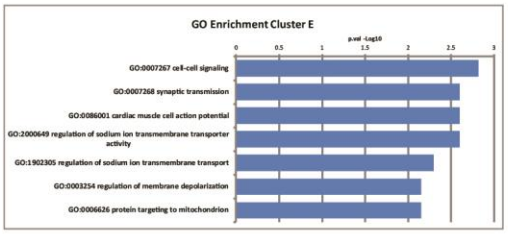
GO Enrichment Cluster E
p.val -Log10
0 0.5 1 1.5 2 2.5 3
GO:0007267 cell-cell signaling
GO:0007268 synaptic transmission
GO:0086001 cardiac muscle cell action potential
GO:2000649 regulation of sodium ion transmembrane transporter activity
GO:1902305 regulation of sodium ion transmembrane transport
GO:0003254 regulation of membrane depolarization
GO:0006626 protein targeting to mitochondrion

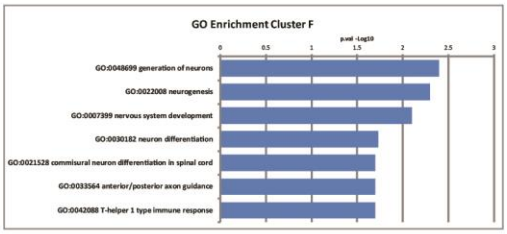
GO Enrichment Cluster F
p.val -Log10
0 0.5 1 1.5 2 2.5 3
GO:0048699 generation of neurons
GO:0022008 neurogenesis
GO:0007399 nervous system development
GO:0030182 neuron differentiation
GO:0021528 commisural neuron differentiation in spinal cord
GO:0033564 anterior/posterior axon guidance
GO:0042088 T-helper 1 type immune response

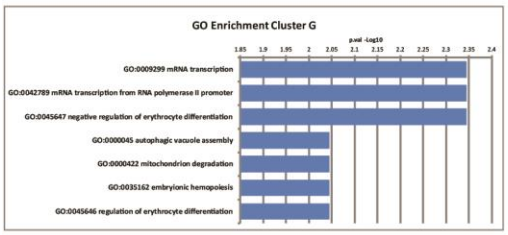
GO Enrichment Cluster G
p.val -Log10
1.85 1.9 1.95 2 2.05 2.1 2.15 2.2 2.25 2.3 2.35 2.4
GO:0009299 mRNA transcription
GO:0042789 mRNA transcription from RNA polymerase II promoter
GO:0045647 negative regulation of erythrocyte differentiation
GO:0000045 autophagic vacuole assembly
GO:0000422 mitochondrion degradation
GO:0035162 embryonic hemopoiesis
GO:0045646 regulation of erythrocyte differentiation

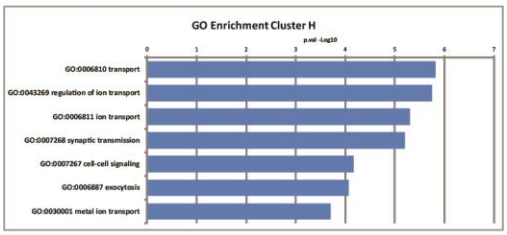
GO Enrichment Cluster H
p.val -Log10
0 1 2 3 4 5 6 7
GO:0006810 transport
GO:0043269 regulation of ion transport
GO:0006811 ion transport
GO:0007268 synaptic transmission
GO:0007267 cell-cell signaling
GO:0006887 exocytosis
GO:0030001 metal ion transport

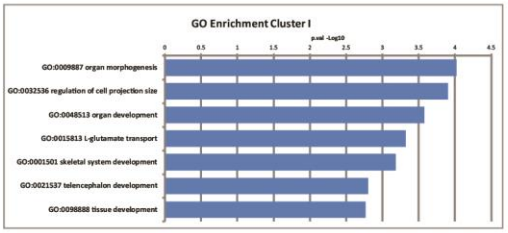
GO Enrichment Cluster I
p.val -Log10
0 0.5 1 1.5 2 2.5 3 3.5 4 4.5
GO:0009887 organ morphogenesis
GO:0032536 regulation of cell projection size
GO:0048513 organ development
GO:0015813 L-glutamate transport
GO:0001501 skeletal system development
GO:0021537 telencephalon development
GO:0098888 tissue development


GO Enrichment Cluster J
p.val -Log10
0 0.5 1 1.5 2 2.5 3
GO:0006607 NLS-bearing protein import into nucleus
GO:0006467 protein deacetylation
GO:0016575 histone deacetylation
GO:0031063 regulation of histone deacetylation
GO:0090311 regulation of protein deacetylation
GO:0031056 regulation of histone modification
GO:0032330 regulatio of chondrocyte differentiation

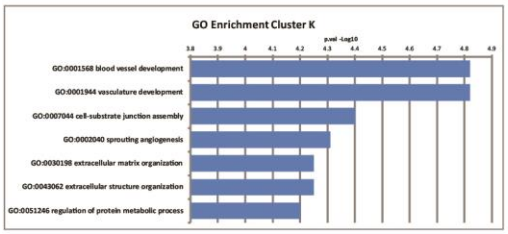
GO Enrichment Cluster K
p.val -Log10
3.8 3.9 4 4.1 4.2 4.3 4.4 4.5 4.6 4.7 4.8 4.9
GO:0001568 blood vessel development
GO:0001944 vasculature development
GO:0007044 cell-substrate junction assembly
GO:0002040 sprouting angiogenesis
GO:0030198 extracellular matrix organization
GO:0043062 extracellular structure organization
GO:0051246 regulation of protein metabolic process

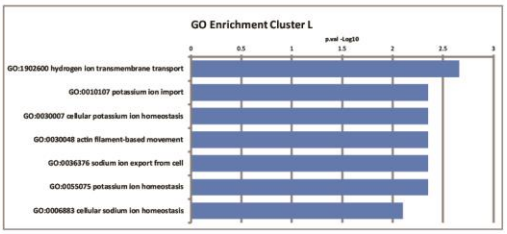
GO Enrichment Cluster L
p.val -Log10
0 0.5 1 1.5 2 2.5 3
GO:1902600 hydrogen ion transmembrane transport
GO:0010107 potassium ion import
GO:0030007 cellular potassium ion homeostasis
GO:0030048 actin filament-based movement
GO:0036376 sodium ion export from cell
GO:0055075 potassium ion homeostasis
GO:0006883 cellular sodium ion homeostasis

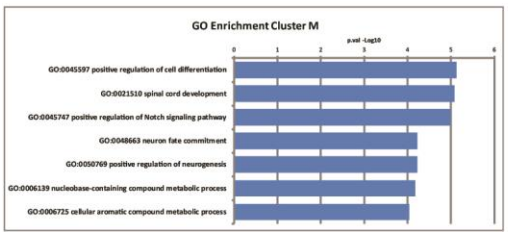
GO Enrichment Cluster M
p.val -Log10
0 1 2 3 4 5 6
GO:0045597 positive regulation of cell differentiation
GO:0021510 spinal cord development
GO:0045747 positive regulation of Notch signaling pathway
GO:0048663 neuron fate commitment
GO:0050769 positive regulation of neurogenesis
GO:0006139 nucleobase-containing compound metabolic process
GO:0006725 cellular aromatic compound metabolic process

Supplementary Figure 4

GO enrichment of common striatal genes.

GO enrichment graphs of lowest p-value categories for each cluster depicted in Figure. 4a, values are in –Log10. For GO enrichment, hypergeometric test was used with p-value < 0.05 adjusted with Benjamini-Hochberg correction.

a

Categories	Diseases or Functions Annotation	Predicted Activation State	Activation z-score	p-Value
Nervous System Development and Function	development of neurons	Decreased	-2.147	1.46E-46
	neurotransmission	Decreased	-2.387	6.26E-30
	synaptic transmission	Decreased	-2.603	1.11E-27
	synaptic transmission of cells	Decreased	-2.565	4.89E-15
	memory	Decreased	-2.887	1.15E-14
	coordination	Decreased	-5.523	1.35E-12
	long-term potentiation	Decreased	-3.811	2.31E-12
	guidance of axons	Decreased	-2.219	6.63E-12
	long-term potentiation of synapse	Decreased	-2.652	1.62E-09
	prepulse inhibition	Decreased	-2.664	3.74E-09
	plasticity of synapse	Decreased	-2.592	8.45E-09
	transport of synaptic vesicles	Decreased	-2.208	2.45E-07

Categories	Diseases or Functions Annotation	Predicted Activation State	Activation z-score	p-Value
Behavior & Nervous System Development and Function	behavior	Decreased	-3.575	6.90E-44
	learning	Decreased	-3.183	6.76E-25
	memory	Decreased	-2.887	1.15E-14
	cognition	Decreased	-2.863	1.06E-23
	conditioning	Decreased	-2.714	1.25E-09
	emotional behavior	Decreased	-2.128	5.33E-17

b

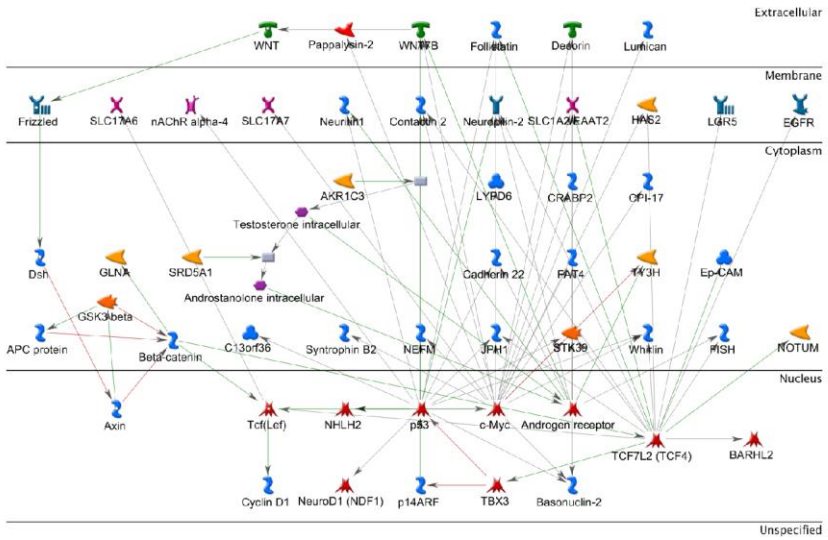

c

Striatal/Striatal	MSN 1869 Genes
Upstream Regulator	Targets
A2M	CDH2,CHAT,FOXO1,GAP43,GRIN1,PRLR,SLC40A1,WNT10B,WNT5A
ACVRL1	CXCL12,EFNB2,ENG,MYC,PLAT,PLAU,PXN,VEGFA
COL18A1	ANTXR1,CD34,CDC25B,EDN1,EFNB2,EPHB1,EPHB4,ETS1,F2RL1,FN1,HIF1AN,ID3,IL6, ITGB3,MMP2,MYC,PLAU,PTGS2,THBS1,TNFRSF1A,VEGFA
FST	ATP1A2,FABP3,FN1,FSHR,FST,GNRH1,IL6,MMP2,MSTN,PRLR
IGF2BP1	CD44,COL14A1,COL5A1,COL6A3,LGALS1,LIN28B,LUM,MYC,SERPINH1
ITGA5	CD44,CDH2,CHRD,ENPP2,ERBB2,GAS1,MMP14,MMP2,PLAU,PTGER4,PXN,TGFBR2
MAPK1	ANPEP,APBB3,ATP1A2,ATP1B1,BCL11A,CDH2,CDK5R1,CRABP2,CTNNA2,DEPTOR,DG KI,DLX3,DSE,DUSP1,FLNC,FN1,GBP5,GFOD1,GNG2,GRB7,HOXA11,IL6,ITGB3,LGALS 1,LMNA,MMP2,MVP,NRN1,OLFML2A,PDGFB,PDLIM3,PITX2,PLAU,PLD1,POU2F2,PR KG1,PTGS2,RFPL1/RFPL3,SCNN1A,SFRP2,SNAI1,SOCS2,SPP1,TP53,TRIM38,VDR
NHLH2	ADRB2,ASCL1,GNRH1,IL6,PCSK1,TRH
PECAM1	CD44,IL6,MMP2,THBS1
SMAD6	DNMT3B,IL6,SPP1,TGFB3

Supplementary Figure 5

RNA-seq functional subcategories, interaction map of common striatal genes, and table of genes that regulate human striatal maturation and HD differential gene expression.

(a) RNA-Seq functional subcategories under the super-category nervous system development and function. Select categories listed are predicted to be decreased by calculation of activation z-score. P-value calculated by Fisher's exact test of expected/observed genes found within specific subcategories. Predicted state of subcategories shows a decrease in neuronal development and function, including: synaptic transmission, long-term potentiation, guidance of axons, and organismal effects to learning and memory. (b) Interaction map: Largest connected Network by Direct Interaction sets in Metacore ® platform, derived from Cluster I in Figure S4. Green lines represent activation red lines inhibition. (c) 1869 DEGs from RNAseq analysis between HD and non-diseased differentiated iPSCs were compared to genes involved in human striatal maturation. Genes relevant to human striatal maturation were also genes predicted to be upstream regulators of the DEGs found in the HD versus non-diseased iPSC-derived samples.

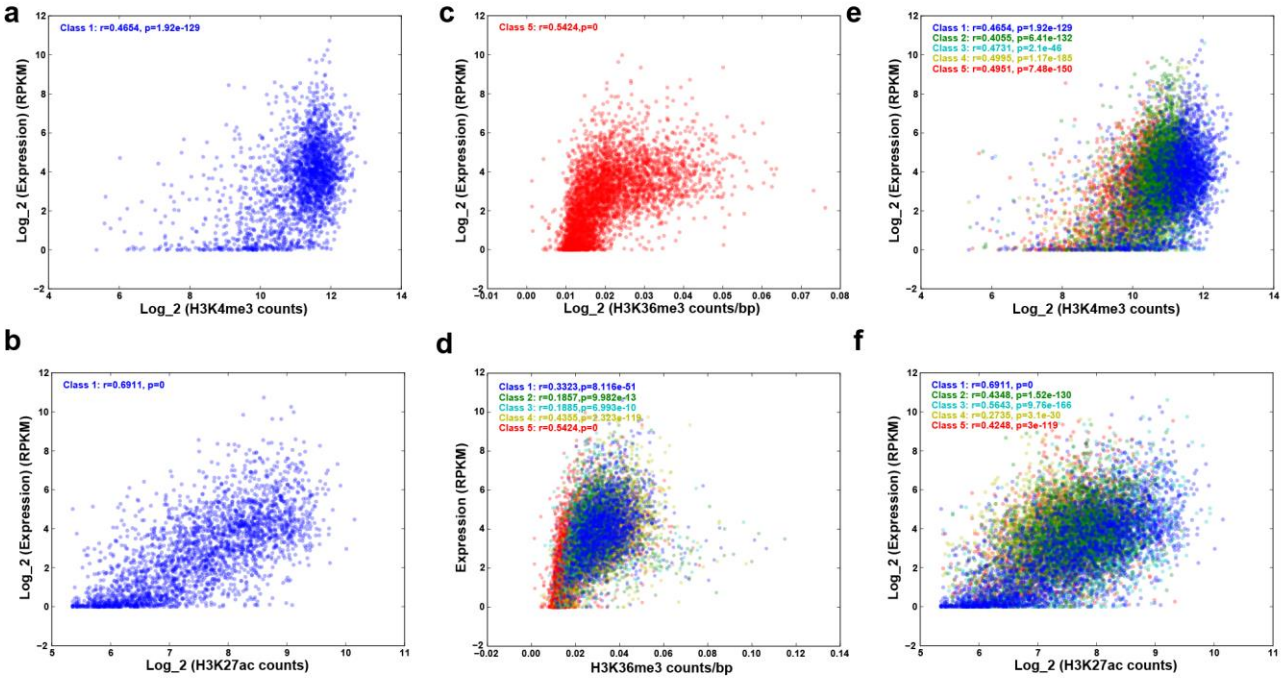

g

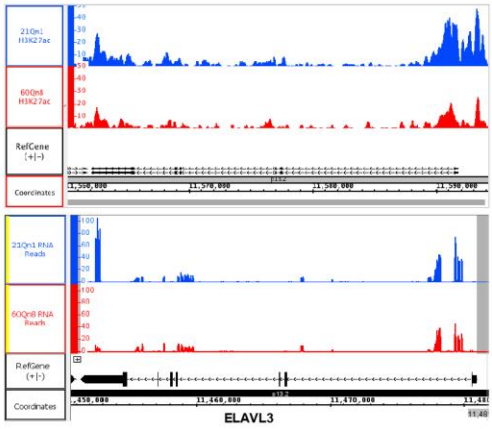

h

Control Enriched

Motif Names	Motif	p value
ZNF219, KROX	.gctGaGtCA.	7.03E-108
Sp1, CKROX, Sp4	..gGGGcGGgg..	1.47E-81
p53, p63	rr.OwwGycyrrrCwwGyyy	4.56E-42
ZNF515, Pax-4, Zic1, Zic2, Zic3, LF-A1, LRF	.wwTAAGTAtwt	5.82E-34
E2F1	tTTsGCGsg	1.18E-32
MAZR, MOVO-B, WT1	.TCCTGCA.	1.99E-32
HIC1	...ggkTGCccss.g..	9.67E-32
FPM315	rCCmCrCCCw..	1.08E-31
AP-2	...TTGc..aa...	1.40E-30
MAZ, Zfp281	.rrGCTCgCy..	2.65E-30

HD Enriched

Motif Names	Motif	p value
FOXD3, HNF3a, HFH4, FOX	AATwtTYaMCAG	4.21E-19
MEF2, RSRFC4	..tGTTaCTAWAAATAGaam..	3.62E-18
Irx2, Irx3, Irx4, Irx5	.c..aTAATTA.m..c	1.21E-14
HNF1, HP1	.....TrTTtrytyw...	2.79E-14
MEF2A, MEF2	mrgCArCwGswG	1.09E-13
Nkx2-2, Nkx2-3	a..cGcTGTwaw....	4.02E-13
RP58, TAL1	...rmCAGATGkT...	9.51E-13
Nkx6-2, Pax-4	.....yCACccs	1.04E-12
FOXO3, Freac-3, Freac-4, FOXJ2, HNF3	ts.gycATTA.....	1.40E-12
FOXO4, FOXO1, SRY	g..TTGTTTACt.y	2.24E-12

i

TFs with motifs under HD-biased peaks	FDR	TFs with motifs under Ctrl-biased peaks	FDR
dna-binding	1.12E-102	Transcription	6.36E-54
Homeobox	6.99E-59	regulation of transcription	6.56E-43
regulation of transcription from RNA polymerase II promoter	1.85E-38	regulation of transcription from RNA polymerase II promoter	1.58E-26
transcription factor complex	5.44E-26	zinc finger region:C2H2-type 1	7.57E-24
Winged helix repressor DNA-binding	5.27E-17	negative regulation of gene expression	8.76E-11
negative regulation of transcription, DNA-dependent	6.66E-11	nuclear lumen	1.83E-12
pattern specification process	2.56E-18	transcription, DNA-dependent	0.00014
transcription from RNA polymerase II promoter	1.45E-09	transcription factor binding	1.62E-05
chordate embryonic development	9.90E-09	cross-link:Glycyl lysine isopeptide (Lys-Gly)	2.21E-05
cross-link:Glycyl lysine isopeptide (Lys-Gly)	2.94E-08	chromosomal part	0.0111
regulation of gene-specific transcription	9.54E-06	regulation of gene-specific transcription	0.000289
domain:Leucine-zipper	3.15E-11	embryonic morphogenesis	2.24E-05
forebrain development	3.98E-05	Basic helix-loop-helix dimerisation region bHLH	0.000262
Zinc finger, NHR/GATA-type	5.97E-06	lung development	0.0101
nucleolus	0.000152	chromatin binding	0.000624
Iroquois-class homeodomain protein	0.0107	zinc finger region:C2H2-type 6	7.21E-06
DNA-binding region:Tryptophan pentad repeat	0.0337	tube development	0.0122
regulation of nervous system development	0.0264	promoter binding	0.00032
urogenital system development	6.43E-08		
reproductive developmental process	0.000359		

Supplementary Figure 6

RNA-seq and ChIP-seq correlation plots, differential peak height, motif analysis and GO analysis.

(a-c) The number of ChIP-Seq read counts mapped to the area around gene transcription start sites (-2kb up to +3 kb) was correlated with the expression level of that gene according to RNA-Seq. Data are for the 21Qn1 cell line, for all genes in HD-associated epigenetic classes. Pearson r and two-tailed p values are shown. Read counts were calculated after normalizing data with FIXSEQ (82). (d-f) The number of ChIP-Seq read counts mapped to the area around gene transcription start sites was correlated with the expression level of that gene, according to RNA-Seq for genes in all epigenetic classes. (g) The number of H3K27Ac ChIP-Seq reads and RNA reads mapped to the area of the human genome around *ELAVL3*, a neuron-specific ribosome binding protein that is down regulated in HD.

Reads from the 21Qn1 non-disease cell line (top) and 60Qn8 HD line (bottom) are shown. Using k-means clustering of the peak profile of *ELAVL3* was assigned to class 1, with its broad peak extending into the gene body from the TSS. Reads were visualized using Integrated Genome Browser. (h) The top 10 motifs found under H3K27ac peaks enriched in HD versus non-disease samples are shown. Motifs were clustered according to similar binding site sequences. The left column shows all members of a cluster, the middle column shows an example binding site for that cluster, and the third column shows the p-value of enrichment of the best member of that motif cluster over the peaks enriched in the opposite treatment group. (i) Gene Ontology categories assigned to enriched transcription factor motifs in HD or non-disease samples and false discovery rate adjusted p-value.

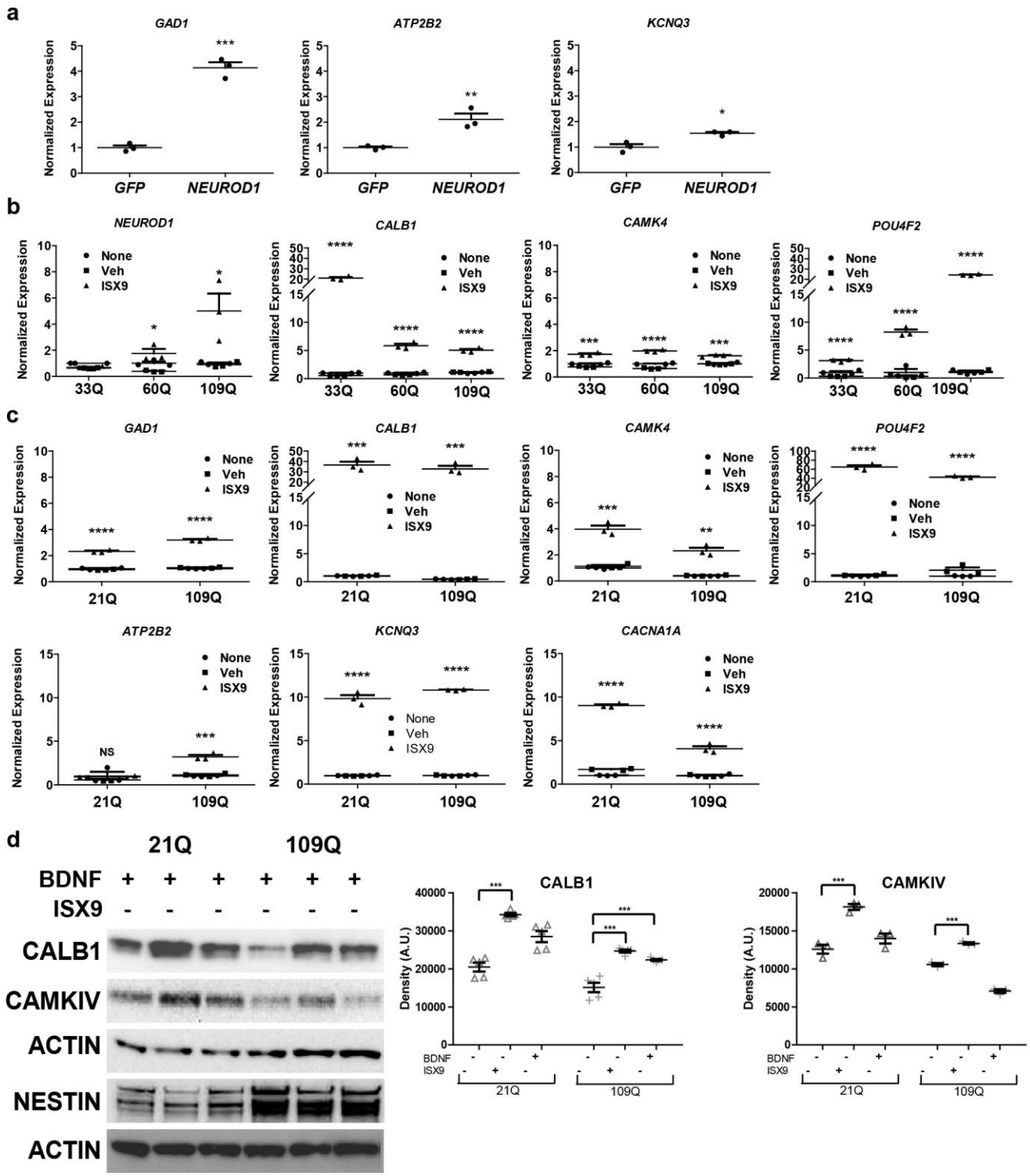

Supplementary Figure 7

NEUROD1 overexpression and Isx-9 increase expression of downregulated transcripts.

(a) NEUROD1 over-expression enhances neuronal gene expression in high CAG repeat lines. Several genes in addition to those depicted in Figure 6 were evaluated in the high CAG repeat HD line 109Q after either human NEUROD1 overexpression lentivirus or pFUGW-eGFP. qPCR demonstrates increased expression of *GAD1* (P=0.0002, t=13.20, df=4), *ATP2B2* (P=0.0087, t=4.790, df=4) and

KCNQ3 (P=0.0121, t=4.352, df=4). (b) Isx-9 enhances expression of *NEUROD1* (33Q: P=0.4290, t=0.879, df=4; 60Q: P=0.0173, t=3.92, df=4; 109Q: P=0.0374, t=3.066, df=4) and other neuronal genes *POU4F2* (33Q: P<0.0001, t=19.95, df=4; 60Q: P<0.0001, t=16.49, df=4; 109Q: P<0.0001, t=51.96; df=4), *CAMK4* (33Q: P=0.0002, t=13.45, df=4; 60Q: P<0.0001, t=24.01, df=4; 109Q: P=0.0004, t=10.98, df=4) and *CALB1* (33Q: P<0.0001, t=19.00, df=4; 60Q: P=0.0001, t=15.36, df=4; 109Q: P<0.0001, t=17.18, df=4) in non-disease (33Q) and HD cultures (60Q, 109Q). (c) Additional genes were tested in 21Q and 109Q lines with increased expression of *GAD1* (21Q: P<0.0001, t=21.86, df=4; 109Q: P<0.0001, t=27.90, df=4), *CALB1* (21Q: P=0.0004, t=10.72, df=4; 109Q P=0.0004, t=11.19; df=4), *CAMK4* (21Q: P=0.0007, t=9.628, df=4; 109Q: P=0.0011, t=8.390, df=4), *POU4F2* (21Q: P<0.0001, t=16.32, df=4; 109Q: P<0.0001, t=25.26, df=4), *KCNQ3* (21Q: P<0.0001, t=21.84, df=4; 109Q: P<0.0001, t=168.1, df=4) and *CACNA1A* (21Q: P<0.0001, t=50.08, df=4; 109Q: P=0.0005, t=10.19, df=4) in all cultures, as well as increased expression of *ATP2B2* in the HD 109Q line (21Q: P=0.0548; t=2.688, df=4; 109Q: P=0.001, t=8.618, df=4). For qPCR analysis, a statistical difference in gene expression between GFP and NEUROD1 overexpression or vehicle and Isx-9 treatment was determined using an unpaired two-tailed t-test in GraphPad Prism. (d) Isx-9 western analysis. 21Q and 109Q cell lines demonstrate increased protein expression of CALB1 and CAMKIV after Isx-9 treatment. WB results (densitometry) were normalized to ACTIN. Statistical significance between Isx-9 and untreated cells (NIM) was determined by one-way ANOVA. CALB1: 21Q plus ISX9 (P=0.0001, n = 5 independent differentiations, df=1, F=123.59). 109Q plus ISX9 (P=0.0001, n=5 independent differentiations, df=1, F=54.11). 109Q plus BDNF (P=0.000457, n=5 independent differentiations, df=1, F=32.43). CAMKIV: 21Q plus ISX9 (P=0.001359, n=3 independent differentiations, df=1, F=63.12). 109Q plus ISX9 (P=0.000337, n=3 independent differentiations, df=1, F=130.03). Full blots in S8.

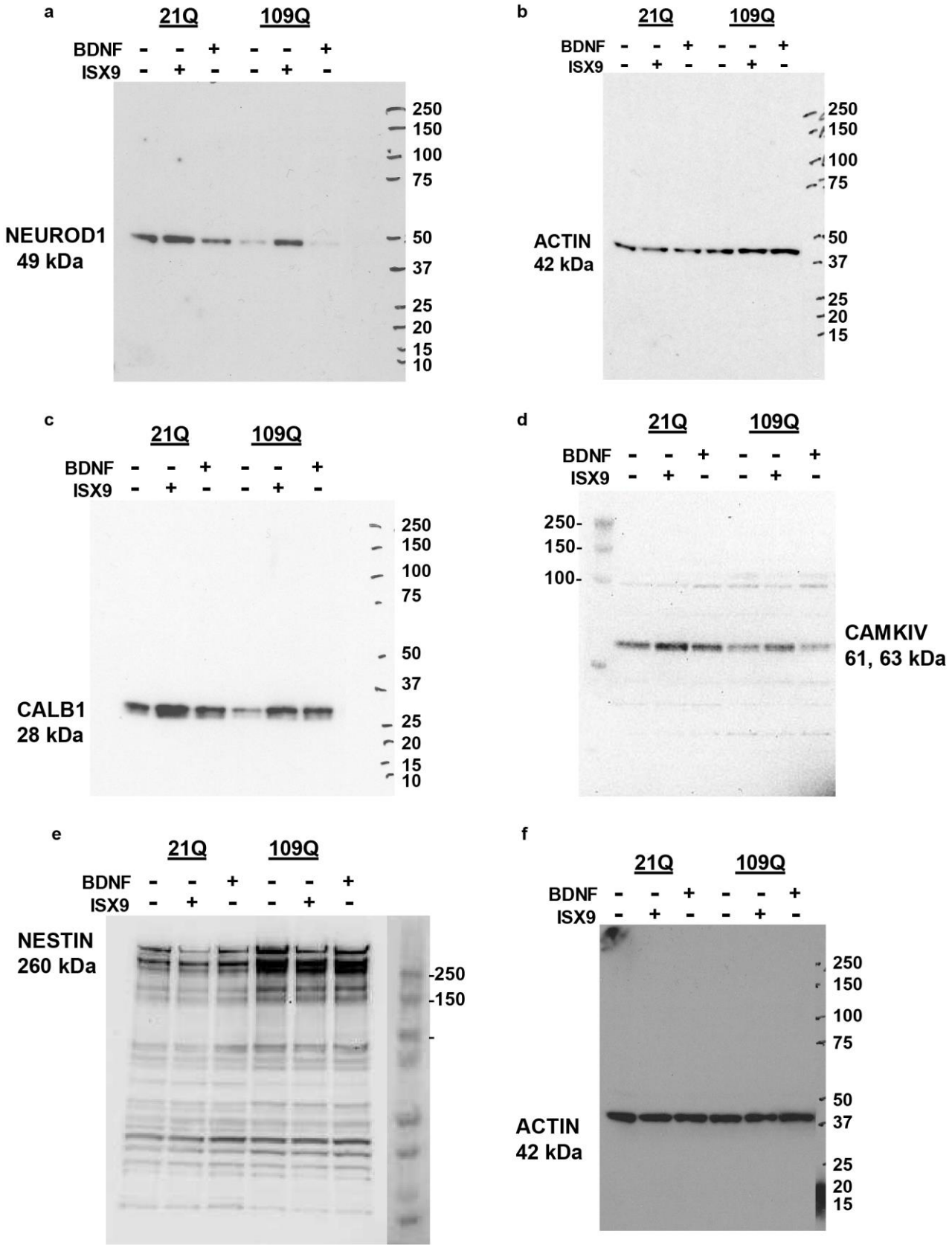

Nature Neuroscience: doi:10.1038/nn.4532

Supplementary Figure 8

Full western blots with original markings

Full scanned gels for western blots shown in figures 6d (a-b) and S7d (b-f). Some gel images were cropped to merge mw markers with protein bands while removing samples unrelated to study which were ran on the same gel.

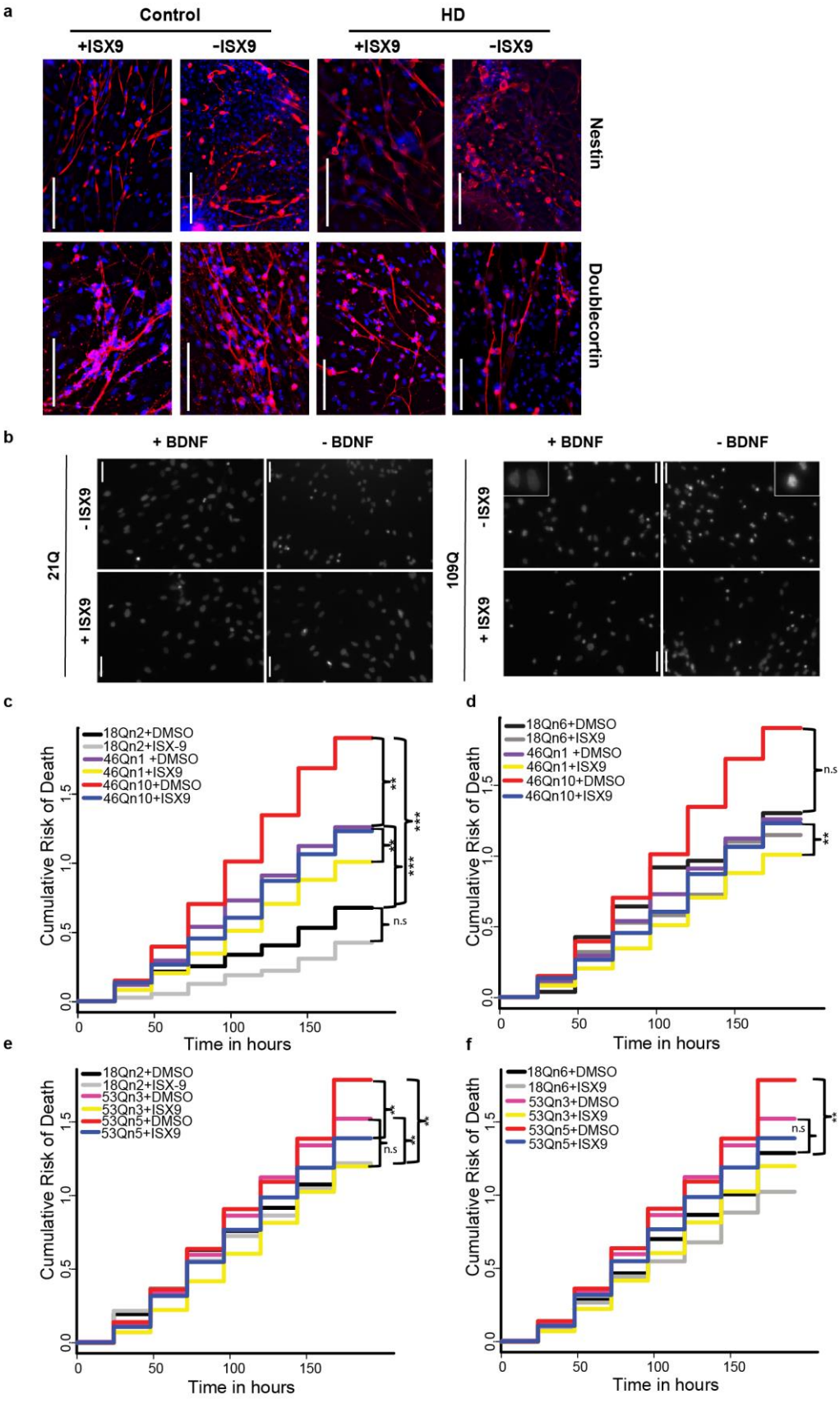
a
Control
HD
+ISX9
-ISX9
+ISX9
-ISX9
Nestin
Doublecortin
b
+ BDNF
- BDNF
+ BDNF
- BDNF
21Q
109Q
- ISX9
+ ISX9
- ISX9
+ ISX9
c
18Qn2+DMSO
18Qn2+ISX-9
46Qn1 +DMSO
46Qn1+ISX9
46Qn10+DMSO
46Qn10+ISX9
Cumulative Risk of Death
Time in hours
n.s
d
18Qn6+DMSO
18Qn6+ISX9
46Qn1 +DMSO
46Qn1+ISX9
46Qn10+DMSO
46Qn10+ISX9
Cumulative Risk of Death
Time in hours
n.s
e
18Qn2+DMSO
18Qn2+ISX-9
53Qn3+DMSO
53Qn3+ISX9
53Qn5+DMSO
53Qn5+ISX9
Cumulative Risk of Death
Time in hours
n.s
f
18Qn6+DMSO
18Qn6+ISX9
53Qn3+DMSO
53Qn3+ISX9
53Qn5+DMSO
53Qn5+ISX9
Cumulative Risk of Death
Time in hours
n.s

Supplementary Figure 9

HD and control neural cells show no difference in cell composition after Isx-9 treatment; representative pictures used for nuclear condensation assay; and cumulative risk of death for adult-onset-range differentiated iPSCs.

(a) Immunocytochemistry at day 56 of differentiation demonstrate that both HD and non-disease iPSC lines can generate neural progenitors (NESTIN, DOUBLECORTIN). Scale bar represents 100 um.(b) Differentiated iPSC cultures were treated with ISX-9 or BDNF for 48 h. Nuclei were stained with Hoechst 3343. The images were obtained on an Axiovert 200 inverted microscope and quantified using Volocity. Representative images are show for each condition. Inserts illustrate healthy nuclei (left panel) and condensed nuclei (right panel). (c) The cumulative risk of death of both the 46Qn1 (HR= 2.1, p= 4.16e-06) and 46Qn10 (HR= 2.9, p= 0.000243) are greater than the control 18Qn2 line. Addition of 20 µM ISX-9 decreases the cumulative risk of death of 46Qn1 (HR= 0.79, p= 0.004961) and in the 46Qn10 (HR=0.65, p= 5.42e-06). (d) Although we saw a trend in the survival curve of the 46Qn10, we did not see significant differences in the CRD between the 18Qn6 risk of death to the 46Qn1 (HR= 0.87, p= 0.4) and the 46Qn10 (HR= 1.2106, p= 0 0.367148) likely due to a low n as when we combine clones the difference becomes significant as in Figure 7. Control 18Qn2 +DMSO, n=69 cells, Control 18Qn +ISX-9, n= 78 cells, Control 18Qn6+DMSO, n=55 cells, Control 18Qn6+ISX-9, n= 66 cells, (n=2 experiments). 46Qn1 + DMSO, n= 414 cells, 46Qn1+ISX-9, n= 474 cells, (n=5 experiments); 46Qn10+DMSO, n= 289 cells, 46Qn10+ISX-9 n= 310 cells, (n=5 experiments). (e) We evaluated the cumulative risk of death of the 53Qn3 lines compared to the controls. We found evidence of non-proportionality for a subset of the lines so we used log rank tests to assess the differences of survival between the HD and controls lines and the effects of ISX-9 on the HD and control lines. All p values are reported from the log rank test; however, we report the hazard ratios as an estimate of the hazard from the Cox proportional hazards model. (f) The cumulative risk of death of the 18Qn2 is lower risk of death than the 53Qn3 (HR= 1.4, p= 0.06 approaching significance) and 53Qn5 (HR=1.3 p= 0.00572). Addition of 20 µM ISX-9 increases survival of 53Qn3 (HR= 0.74, p= 2.4e-06) and 53Qn5 (HR=0.83, p= 0.0198) i-neurons. ISX-9 does not significantly change cumulative risk of death for the control Q18n2 (p= 0.931). The cumulative risk of death of 18Qn6 is lower than the 53Qn3 (HR= 1.2, p= 0.0535 approaching significance) and 53Qn5 (HR=1.3, p= 0.00622). ISX-9 does not significantly change cumulative risk of death for the control Q18n6 (p= 0.197). Control 18Qn2 +DMSO, n=345 cells, 18Qn +ISX-9, n= 324 cells, (n=4 experiments) Control 18Qn6+DMSO, n=145cells, 18Qn6 + DMSO, n= 128 cells, (n=3 experiments); 53Qn3+DMSO, 695 cells, 53Qn3+ISX-9, n= 726 cells, (n=6 experiments); 53Qn5+DMSO, 352 cells, 53Qn5+ISX-9, 381cells (n=3 experiments).

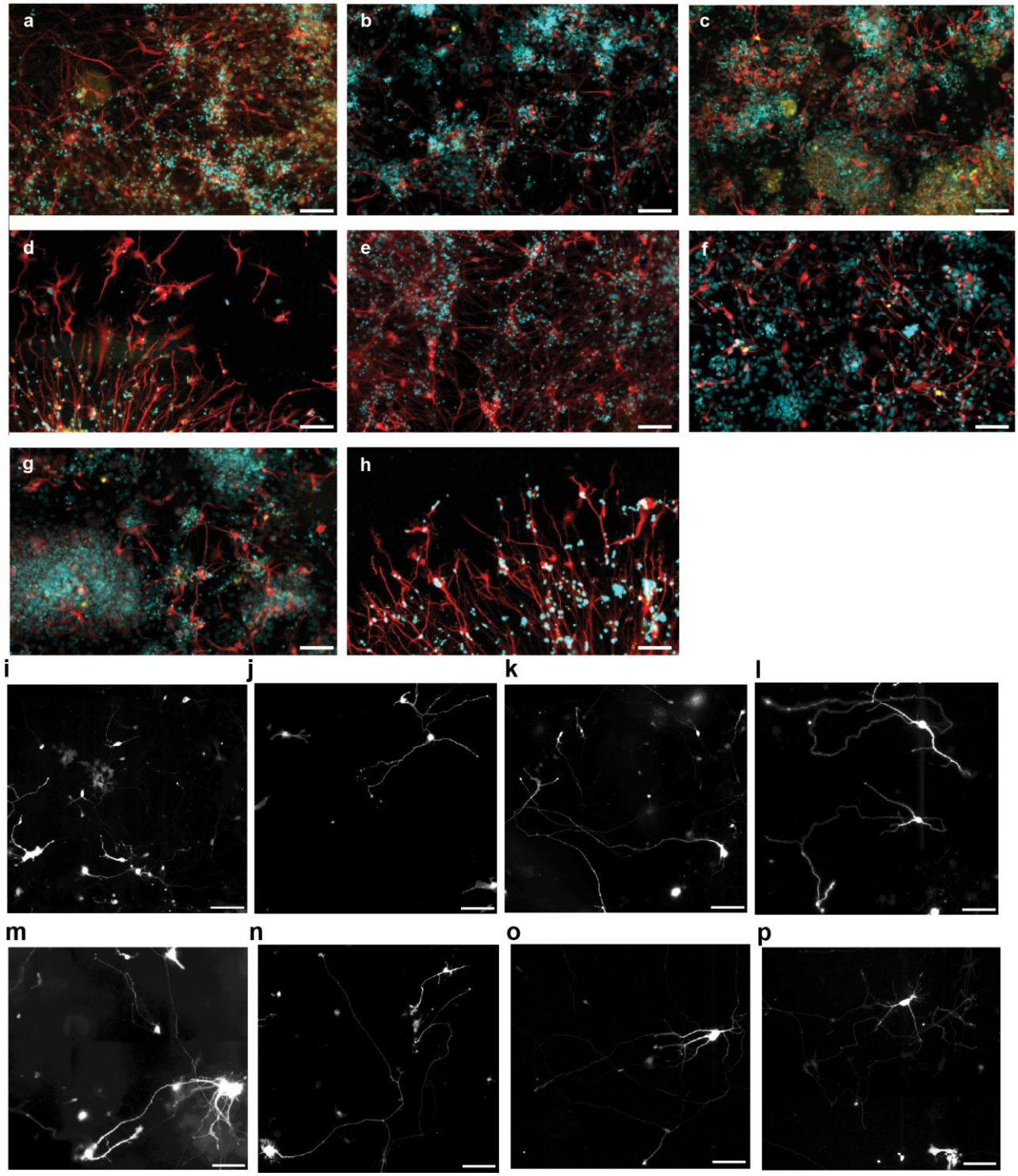

Supplementary Figure 10

Representative images of immunocytochemistry staining of differentiated cells that were used in robotic microscopy for survival and neurite-like process length analysis, and representative images of neurons that were subjected to neurite-like length analysis.

(a-h) Cells stain for ~5-15% DARPP-32 positive cells and ~1-15 % Ki67 cells. To determine percent of cells staining for DARPP-32 or Ki67, we subjected the DAPI nuclear stained images to our custom plugin in ImageJ to create an ROI for each cell. The images were processed, thresholded, and masked. These masks subjected to particle analysis that constraints size and shape to reduce the

measuring of artifacts. The masked ROIs were overlayed on to the green channel images and pixels were measured for fluorescent intensity and size. The average intensity values were normalized to the size of the nuclei, and only the nuclei with a value or 0.2 or greater were counted as significant. The number of positive staining nuclei (cyan, blue channel) was divided by total number of nuclei to determine the percentage of KI-67 and DARPP-32 positive cells. MAP-2 (red, red channel) and DARPP-32 (yellow, green channel) staining (a,c, e, g) and staining for MAP-2 (red) and Ki67 (b, d, f ,h), of the (a, b) control 28Q, (c, d) 46Q (c, g) 53Q and (e, f) 109Q. Scale bar is 100 µm. (i-p) Example images of cells analyzed for process length, (i) 18Qn2, (j) 28Qn6 (k) 46Qn1 (l) 46Qn10 (m) 53Qn3 (n) 53Qn5 (o) 109n4 (p) 109Qn5. Scale bar is 100 um.

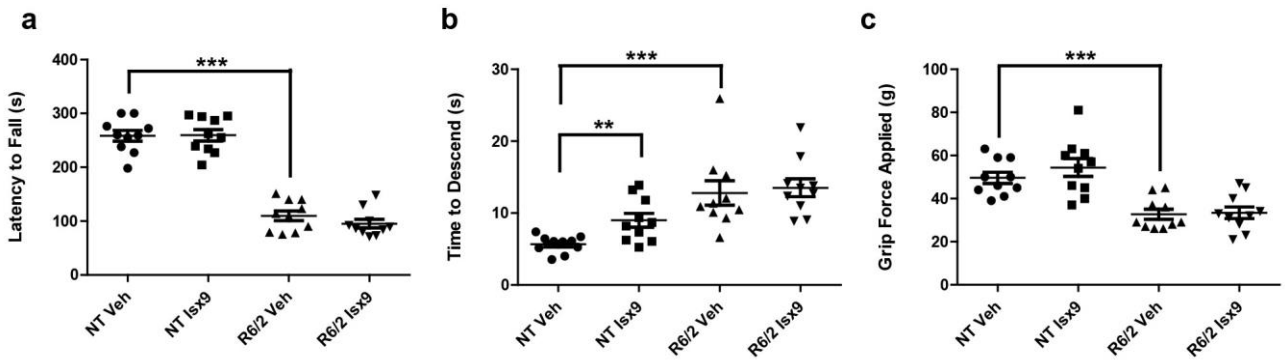

Supplementary Figure 11

Motor behaviors are not rescued by Isx-9 treatment in R6/2 mice.

Mice were initially tested for specific HD related behavior deficits using tasks that examine motor impairment. Genotype effects were observed by 8 weeks; however, Isx9 did not provide statistically significant differences in treated versus control mice in rotarod (a) pole test (b) or grip strength (c) assays. (a) Rotarod indicates no motor improvements in Isx-9 treated mice. Non-transgenic (NT) and R6/2 mice treated with vehicle (veh) or Isx-9 were subjected to the rotarod task to evaluate motor ability. Impairment was observed in R6/2 mice. Points represent individual mouse scores of time on rotarod measured in seconds. Center lines represent mean of each groups data set and error bar whiskers are indicative of SEM (n=10/group at 8 weeks age). Statistical tests used one-way ANOVA followed by Tukey HSD Test with Scheffé, Bonferroni and Holm multiple comparison calculation also performed post hoc. One-way ANOVA F value 92.8 with 3 degrees of freedom, ***p=0.001. (b) Pole test indicates no motor improvements in Isx-9 treated R6/2 mice. Non-transgenic (NT) and R6/2 mice treated with vehicle (veh) or Isx-9 were subjected to the pole test task to evaluate motor ability. Impairment was observed in R6/2 mice. Points represent individual mouse scores of time to descend measured in seconds. Center lines represent mean of each groups data set and error bar whiskers are indicative of SEM (n=10/group at 9 weeks age). Statistical tests used one-way ANOVA followed by Tukey HSD Test with Scheffé, Bonferroni and Holm multiple comparison calculation also performed post hoc. One-way ANOVA F value 9.7 with 3 degrees of freedom, ***p=0.001. (c) Grip strength test indicates no improvements in Isx-9 treated mice. Non-transgenic (NT) and R6/2 mice treated with vehicle (veh) or Isx-9 were subjected to the grip strength task to evaluate forelimb grip. Impairment was observed in R6/2 mice. Points represent individual mouse scores of grip measured in grams of strength. Center lines represent mean of each groups data set and error bar whiskers are indicative of SEM (n=10/group at 10 weeks age). Statistical tests used one-way ANOVA followed by Tukey HSD Test with Scheffé, Bonferroni and Holm multiple comparison calculation also performed post hoc. One-way ANOVA F value 13.6 with 3 degrees of freedom, ***p=0.001.

iPS Cell Line	Clone	Gender	Diagnosis	CAG repeats	Coriell Catalog ID (fibroblasts)	Reference
CS25iCTR18 (18Q)	n2, n6	FEMALE	Clinically normal	18	Submitted, pending	N/A
CS00iCTR21 (21Q)	n1	MALE	Clinically normal	21	GM05400	Sareen et al. (2013, 2014)
CS14iCTR28 (28Q)	n6	FEMALE	Clinically normal	28	GM03814	Sareen et al. (2013)
CS83iCTR33 (33Q)	n1	FEMALE	Clinically normal	33	GM02183	Sareen et al. (2013)
CS04iHD46 (46Q)	n1, n10	MALE	HD	46	Submitted, pending	N/A
CS03iHD53 (53Q)	n3, n5	MALE	HD	53	Submitted, pending	N/A
CS21iHD60 (60Q)	n5, n8	FEMALE	HD	60	GM03621	Mattis et al. (2015)
CS02iHD66 (66Q)	n4	FEMALE	HD	66	Submitted, pending	N/A
CS81iHD71 (71Q)	n3	FEMALE	HD	71	GM04281	N/A
CS09iHD109 (109Q)	n1, n4	FEMALE	HD	109	ND39258	Mattis et al. (2015)

Table S1. Cell line and Patient information

Clinical information on subjects with HD and non-disease controls for generation of non-integrating iPSC lines. Abbreviations: CS–Cedars-Sinai; n(clones)–non-integrating; UK–unknown; N/A–not applicable.; HD–Huntington's disease. All are of Caucasian ethnicity, with the exception of the 21Q non-disease line derived from individual of African American descent.

Gene Symbol	Adjusted p-value	Fold Change
AATK	0.036711827	-2.53
ABAT	0.011918424	-2.56
ABCD2	0.063413899	-2.36
ACADL	0.031382471	6.80
ACHE	0.017760001	-2.61
ACOT7	0.025873824	-2.29
ACSBG1	0.089294738	-2.84
ACTL6B	2.96E-09	-6.22
ACVR2B	0.003342096	-2.35
ADAM11	0.014085633	-2.64
ADAMTS5	0.000733667	3.40
ADAP1	0.016018667	-3.13
ADARB2	0.004180031	-4.49
ADCY5	0.017902873	-2.38
ADORA2A	0.004725399	-3.74
AFAP1L2	0.000989912	2.67
AGAP2	0.033922836	-2.24
AGTPBP1	0.002891596	-2.65
AJUBA	0.003312275	2.77
ALDH1A3	1.65E-12	6.04
ALDOC	2.56E-11	-5.05
AMPH	1.22E-06	-3.94
ANKRD12	0.067212371	-1.94
ANKRD45	0.043996649	-3.09
ANTXR1	0.033403771	2.06
ANTXR2	0.000214251	2.80
ANXA2	0.044295346	1.84
ANXA6	0.024643773	2.05
APBA1	0.007217399	-2.56
APBB2	0.03679557	-2.26
ARC	0.096720174	-3.11
ARHGAP44	0.044498608	-2.34
ARHGDIG	3.00E-05	-7.15
ASB4	0.03817112	7.31
ASCL1	0.029932733	-2.11
ASIC1	0.041364566	-2.13
ASRGL1	0.033922836	-2.58
ATF5	0.000319488	2.78
ATP1A2	0.006969613	-2.55
ATP1A3	4.07E-09	-4.41
ATP1B1	0.029744925	-2.30
ATP1B2	0.018256589	-2.19
ATP2B2	0.01538077	-2.40
ATP6V0E1	0.017866336	1.91
ATP6V1G2	0.002462736	-2.92
ATP8A1	0.034314682	-1.83
ATP8A2	0.014085633	-2.52
ATP9A	0.023729386	-2.43
AVEN	0.088951053	2.65
B3GALNT1	0.003512379	-3.97
B4GALNT1	0.007837688	-2.69
BACH2	0.001049373	-2.72
BAI3	4.28E-05	-3.32
BARHL2	0.051402187	-5.09
BICC1	0.032466956	2.72
BIN1	5.66E-05	3.20
BMP2	0.027630512	2.72
BNC2	1.29E-07	4.67
BOC	0.005475373	2.26
C10orf35	0.000247171	-4.21
C12orf68	0.014397254	-2.47
C16orf45	0.038961265	-2.22
CACNA1A	0.007245581	-2.98
CACNA1B	9.52E-05	-3.49
CACNA1D	0.071687643	-3.43
CACNA1E	4.55E-08	-5.37
CACNB1	0.028324048	2.27
CACNG2	0.031661493	-4.42
CACNG4	0.001794726	-2.53
CADM3	8.57E-05	-3.20
CADPS	6.10E-06	-3.91
CALB1	0.000160447	-4.85
CALCRL	0.029333679	2.25
CALY	5.64E-07	-6.36
CAMK1D	0.044092327	-3.25
CAMK2B	2.60E-07	-4.94
CAMK4	0.006899552	-5.09
CAMKV	5.72E-12	-5.55
CAMSAP3	0.00011519	-3.23
CAMTA1	0.000551943	-2.88
CAND2	0.00663585	2.42
CAP2	6.88E-06	4.06
CBLN4	0.005288494	38.13
CCDC64	0.025253292	-2.93
CCND3	0.065053543	1.74
CD63	0.016752353	2.19
CDC25B	5.22E-05	3.53
CDC42EP2	0.001285043	3.37
CDH11	6.31E-06	3.62
CDH22	5.09E-05	-5.12
CDH6	0.003404122	-2.55
CDH9	0.002319373	-8.73
CDK5R1	1.79E-11	-5.34
CDKL2	0.003579989	-2.83
CDS1	0.002723879	-3.25
CEND1	0.000212033	-4.57
CHD5	1.10E-05	-3.62

Nature Neuroscience: doi:10.1038/nn.4532

CHODL	0.014268223	2.53
CHRNA3	0.002743915	-4.13
CHRNA4	2.10E-05	-3.79
CITED2	0.049240039	-2.01
CKMT1B	0.003730105	-10.85
CLEC2L	0.046198323	-6.73
CLVS2	0.022703812	-3.41
CNIH2	0.031131051	-2.19
CNKSR3	0.01462922	2.30
CNNM1	0.036915053	-3.50
CNPY4	0.063152515	1.68
CNTFR	0.001510362	-2.75
CNTN1	0.027631254	-2.37
CNTN2	3.96E-17	-5.47
CNTNAP5	0.001794726	-2.98
CORO1A	0.002509878	-4.01
COX6B2	4.82E-05	-5.17
CPLX1	0.000268771	-4.28
CRABP2	0.065303478	1.84
CRB1	0.007680179	-2.23
CRHR1	0.055500559	-3.60
CRMP1	0.040217842	-2.52
CRYBG3	1.04E-05	3.88
CSDC2	1.31E-05	-4.25
CSPG5	0.001010745	-2.89
CSRNP3	8.50E-05	-4.12
CTSS	0.036360676	4.02
CTTNBP2	0.027537803	-3.08
CUX2	0.002115216	-3.01
CX3CR1	0.08048561	7.67
CXADR	0.000243314	-2.68
CYBRD1	4.99E-05	3.12
CYP2J2	0.061218153	3.71
CYP46A1	0.017021113	-3.39
DAAM2	0.03686396	1.64
DAB1	0.050450028	-2.92
DCAF6	3.10E-05	119.88
DCK	0.007940021	-2.52
DCLK1	0.001664471	-2.83
DCLK2	0.016766821	-2.26
DCN	1.16E-10	5.28
DDAH1	0.003267482	-2.53
DDX25	0.040413867	-3.16
DENND2A	0.02193309	-2.37
DFNB31	0.013695696	-2.54
DGAT2	0.054458169	-2.88
DIRAS1	0.008069002	-2.41
DISP2	4.74E-06	-4.02
DLG4	0.002333025	-2.73
DLGAP1	0.014341318	-2.66
DLGAP2	0.008602196	-3.15
DLL3	0.000843516	-4.03
DMTN	3.05E-08	-5.06
DMXL2	0.082801034	-1.88
DNAJB5	0.013026964	-2.49
DNAJC6	1.65E-07	-3.63
DNER	0.000515011	-3.20
DNM3	9.00E-06	-3.30
DOCK3	0.000429124	-3.19
DOCK4	0.00094962	-2.67
DOK4	0.012489837	-2.60
DOPEY2	0.0195545	-2.20
DPF1	0.00445933	-4.24
DPP10	0.032957117	-1.95
DRAXIN	0.072973153	-2.47
DSCAML1	1.79E-05	-5.45
DTX1	0.00033048	-3.15
DUSP16	0.001627496	-2.73
DUSP26	3.02E-05	-5.86
E2F8	0.007603063	5.27
ECEL1	0.010575763	2.60
ECT2	0.076060133	-1.97
EFHD2	0.006793925	2.06
EFNA3	0.063252371	-2.19
ELAVL4	1.89E-08	-5.45
ELFN2	3.82E-10	-4.74
ELMO1	0.014965805	-2.69
ELOVL4	0.06255971	-2.16
EMP2	0.054042375	1.75
ENC1	0.002523087	-2.88
ENKUR	0.016988094	-2.71
ENO2	1.86E-07	-5.35
EPB41L1	0.027720035	-2.24
EPB41L4A	0.0741788	-2.21
EPHA4	0.01442405	-2.13
EPHA8	0.001316634	-9.03
EPHB1	0.014397254	-2.06
EPHB4	0.001124429	2.58
ERBB2	0.072136031	1.69
ERC2	0.004231313	-3.12
ETS1	3.17E-05	4.27
EYA4	0.009155499	2.39
FABP3	0.000177461	4.12
FABP7	0.000194762	-3.17
FAIM2	0.057278124	-2.19
FAM155A	0.009969741	-2.76
FAM167A	0.098324	-2.14
FAM169A	0.001219652	-2.82
FAM174B	0.00618964	2.56
FAM189A1	0.028216673	-2.78
FAM19A2	0.000693218	-5.26
FAM49A	0.004180031	-2.82
FAM57B	0.019255736	-2.52
FAM60A	0.085367995	-1.86
FAM81A	0.012795541	-3.30
FAM84A	0.041298309	-2.73
FAM84B	0.000345588	-3.20
FAT3	0.016101035	-1.90

Nature Neuroscience: doi:10.1038/nn.4532

FAT4	0.098454251	1.83
FBLN1	7.15E-05	4.02
FBLN2	0.002409916	2.58
FBN1	1.18E-05	3.74
FBN2	0.001679686	2.76
FBXL7	0.014235078	2.10
FGF11	0.032883856	-2.35
FGF12	0.098454251	-2.26
FGF14	5.85E-05	-7.00
FGL2	0.000218525	5.66
FHDC1	0.046720859	-3.03
FIGN	0.023823375	-2.49
FJX1	0.014397254	-2.21
FKBP14	0.052198826	1.94
FKBP1B	0.096480721	-3.33
FLRT2	0.00199054	2.46
FN1	0.001265957	2.80
FNIP2	0.062096213	-1.91
FOSL2	0.040854324	1.89
FOXO1	0.039647057	1.91
FRMD3	0.001081723	3.74
FRMD6	0.000194267	2.85
FRRS1L	0.077995105	-2.33
FRY	0.033022589	-2.03
FST	2.50E-05	4.75
FSTL1	0.051495568	3.23
FUT9	3.42E-09	-3.78
FXYD7	0.051560463	-2.36
GABBR1	0.073135296	-2.13
GABRB1	0.081684688	-3.43
GABRB3	0.003946501	-2.18
GAD1	2.68E-09	-5.53
GAS1	0.000128059	2.91
GAS2L3	0.017522233	-2.96
GCA	0.011427807	-2.55
GCNT2	0.0023932	-3.39
GDAP1	0.067244458	-2.05
GDPD5	0.003823186	-3.06
GFOD1	0.021497801	-3.39
GIPR	0.042059115	-3.04
GLCCI1	0.072314247	-1.85
GLDC	0.096737528	-1.94
GMDS	0.032392317	2.03
GNAO1	9.70E-10	-4.30
GNAZ	0.000723923	-2.78
GNG2	0.004114124	-2.82
GNG3	6.61E-09	-5.76
GNG4	8.35E-14	-5.71
GNG7	0.036694064	-2.23
GNG8	0.016848145	-9.18
GOLGA7B	1.01E-10	-6.02
GPER1	0.07413982	3.01
GPR139	0.044119793	-10.33
GPR153	0.074835028	1.72
GPR158	1.31E-07	-4.20
GPR21	0.000517019	-101.33
GPR22	0.000128059	-13.47
GPR85	6.16E-06	-4.21
GPX8	3.01E-05	3.13
GREM2	0.003900725	3.18
GRIA1	1.02E-05	-3.54
GRIA2	1.58E-11	-5.02
GRIA4	0.008758467	-3.91
GRIN1	1.13E-09	-9.96
GRIN2B	0.002393606	-2.43
GRN	0.018320864	2.04
GSX2	0.008206541	-12.65
HAS2	1.10E-06	3.83
HBEGF	0.014406204	-3.48
HCN3	1.47E-05	-3.72
HCN4	1.99E-08	-5.25
HECW1	5.09E-05	-5.06
HES5	0.082655667	-3.19
HOOK1	0.046791324	-2.09
HPCA	3.63E-10	-7.20
HPCAL1	0.009298532	-2.56
HPCAL4	3.23E-06	-3.28
HSPA2	0.000120763	4.26
HTR5A	0.001773233	-11.65
HTRA1	0.032315931	1.87
ICA1	0.084401304	-3.33
IGDCC3	0.007493086	-2.75
IGSF9B	0.071687643	-1.99
ILDR2	0.007217131	-3.60
INA	1.17E-08	-4.69
INHA	0.013191375	-5.69
INPP4B	0.000715269	4.02
INPPL1	0.026233049	2.08
INSM1	5.39E-05	-3.83
IQGAP2	0.020011593	-2.55
ITIH5	0.002460161	3.40
JAKMIP1	3.20E-07	-8.59
JAKMIP2	0.061111711	-2.06
JAM3	0.039252939	1.94
JPH1	4.00E-15	9.34
JPH3	0.011564736	-2.48
KATNAL1	0.023731398	-2.22
KCNA6	0.000281089	-3.45
KCNB1	0.081414769	-2.23
KCNB2	0.003255879	-5.99
KCNC2	0.016016119	-3.57
KCNH4	0.002960608	-4.97
KCNH7	0.056621053	-5.04
KCNIP1	0.036051677	-2.21
KCNIP3	0.040413867	1.91
KCNQ2	0.063121268	-2.01
KCNQ3	0.00067795	-6.72
KCTD13	0.001680751	-3.20

Nature Neuroscience: doi:10.1038/nn.4532

KCTD16	0.007985318	-3.02
KDELC1	0.073446611	1.88
KHDRBS2	0.021295571	-3.76
KIAA0319	1.28E-06	-5.56
KIAA0513	0.065050619	-2.00
KIAA1244	0.020420412	-2.41
KIAA1324	0.027323442	-3.35
KIAA1598	0.000369383	-3.31
KIDINS220	0.098592244	-2.09
KIF5A	1.14E-08	-4.05
KIF5C	0.028868512	-2.61
KIFC2	0.048833738	-2.32
KIRREL3	0.009126212	-2.82
KLF5	0.040131512	2.09
KLHL1	8.62E-06	-6.20
KLHL23	0.045389219	-2.22
KNDC1	0.054285586	-2.01
KREMEN1	6.79E-05	3.76
LGALS1	0.003478419	2.25
LGI1	0.017866336	-3.85
LGI2	0.096908076	1.82
LHFP	0.026455545	1.85
LHFPL4	6.69E-13	-5.16
LIMA1	0.027814449	1.81
LIN28B	0.001305	-4.50
LINGO1	0.000887513	-2.99
LIPA	0.038916164	2.19
LIX1	3.50E-05	-3.35
LMO1	0.000327005	-3.88
LMO2	0.086803056	-2.51
LMO3	7.60E-07	-3.55
LMTK3	1.57E-05	-3.80
LOXL1	0.01452933	1.90
LOXL2	4.17E-08	5.92
LPAR1	0.00010994	2.84
LPPR5	0.071499298	-2.24
LRRC55	4.09E-05	-3.41
LRRC7	0.038772185	-2.45
LRRN3	0.008758467	-2.34
LRRTM2	5.95E-09	-4.27
LRRTM3	0.000381025	-3.87
LUM	0.000249947	3.91
LYPD6	0.004153504	-2.54
MAGI2	0.031450312	-2.09
MAML3	0.018639343	-2.10
MAP1LC3A	0.080532788	-2.99
MAP3K9	0.008206541	-2.68
MAPK10	0.025468157	-2.46
MAPRE2	0.059194577	-2.05
MCF2L	0.000171165	-3.32
MCM4	0.071687643	1.83
MCU	0.000660837	2.84
ME3	0.02855835	-3.89
MEF2A	0.040281669	1.97
MEGF10	0.038524242	2.11
MEST	0.015482488	3.10
MFAP2	0.004649134	2.22
MFAP4	0.000369147	5.16
MFNG	0.000627837	-5.92
MGAT4A	0.029702917	-1.99
MME	3.88E-14	8.14
MMP14	0.001081723	3.21
MMP24	4.77E-12	-5.86
MN1	0.034221955	-2.22
MSI1	0.020727253	-2.12
MT3	0.000951382	-5.97
MTMR7	0.000463481	-3.44
MTSS1	0.080931073	-1.99
MYC	0.002684626	2.78
MYO6	0.048496078	-2.08
MYT1	2.06E-11	-5.36
MYT1L	5.62E-16	-6.91
NALCN	0.024643773	-3.61
NAPB	7.20E-08	-4.24
NAV2	0.014610222	-2.32
NAV3	0.003996178	-2.43
NBL1	0.09193553	1.63
NCAM1	0.034634674	-2.13
NCOA1	0.000963608	2.83
NDRG4	0.000618139	-3.43
NECAB2	0.000241791	-3.63
NEDD9	0.031450312	-4.25
NEFM	0.002343291	-3.07
NEGR1	0.004113031	-2.28
NEK7	0.036036065	2.03
NEUROD1	1.40E-16	-14.20
NEUROG2	3.47E-09	-17.37
NFASC	0.000758572	-3.00
NFATC4	0.004860471	2.20
NGEF	0.000268771	-3.73
NHLH2	0.007284009	-5.89
NLGN1	0.084604006	-1.99
NMNAT2	0.000141029	-2.73
NOVA1	0.036421007	-2.31
NPAS3	0.003478419	-2.47
NPNT	0.04976221	2.05
NR3C2	0.001016876	4.17
NRGN	2.27E-10	-7.71
NRN1	0.058030878	-2.15
NRP2	0.026349215	-2.05
NRSN1	6.98E-08	-4.66
NRXN1	0.000368472	-2.67
NRXN2	0.001827511	-2.84
NRXN3	0.001800588	-2.53
NSG1	0.014057492	-3.00
NTM	0.048544065	-2.33
NTNG1	0.019321312	2.19
NTRK2	0.060262516	-2.02

Nature Neuroscience: doi:10.1038/nn.4532

NTSR1	8.10E-08	-13.16
NYAP2	0.000212301	-6.19
OGN	9.45E-07	3.96
OLFM1	2.08E-07	-5.61
OLFML2A	8.04E-07	4.15
OLFML2B	3.47E-09	4.65
OLIG1	0.05939123	-3.02
OLIG2	0.044133948	-3.14
OMD	7.79E-05	5.85
OPCML	0.002879492	-2.72
OPRL1	0.061111711	-2.63
OTX1	0.023114919	-6.48
P4HA3	1.16E-05	3.35
PAK6	5.75E-05	-5.20
PAK7	2.25E-15	-7.42
PAPPA2	9.09E-08	5.81
PAQR3	0.026896863	-2.23
PAQR9	0.044532245	-5.67
PARVA	0.014533076	2.16
PCDH17	0.00087321	-2.48
PCDH9	0.023524892	-1.86
PCP4L1	2.36E-14	-10.10
PDE1B	0.099208597	-2.24
PDE2A	0.000122375	-3.59
PDE4A	0.020791943	-2.33
PDE7B	0.003512379	2.59
PDGFRA	0.058168121	1.68
PDGFRL	3.45E-15	9.11
PDK1	5.29E-06	-3.66
PDK4	0.027970741	2.21
PDLIM4	0.003478419	2.04
PDXP	0.040854324	-2.16
PEA15	0.016427606	-3.44
PFKFB3	0.052482853	-2.23
PFKP	0.001263431	-2.89
PGBD5	0.040393581	1.83
PHLDB2	0.057750387	1.93
PHYHIP	0.009182937	-3.05
PKDCC	0.013746725	1.94
PKIA	0.006689146	-2.51
PLCB1	0.089745678	-1.90
PLCH1	0.046198323	-2.07
PLCXD2	0.08518509	-3.28
PLD1	0.052286126	2.28
PLEKHH2	0.097003796	1.65
PLXNB1	0.077070837	-1.99
PMEPA1	0.039160284	1.80
PMP22	0.023166751	2.68
PNMA2	0.023307905	-2.28
POU3F3	4.31E-05	-3.60
PPAP2B	0.00445933	2.55
PPFIA2	4.31E-10	-6.39
PPFIA3	0.000725164	-3.00
PPIC	0.068517144	1.67
PPP1R14A	0.025590325	-8.10
PPP1R14C	0.007524571	-2.51
PPP1R16B	3.08E-06	-4.72
PPP2R2B	0.000178323	-3.35
PPP2R2C	1.02E-06	-3.64
PPP2R5B	0.001371858	-3.01
PRDX6	3.08E-05	3.67
PRKAR2B	5.81E-09	-4.28
PRKCB	0.077913415	-2.56
PRKCZ	0.046808	-2.29
PROX1	0.053744516	-2.04
PRR16	0.001970415	3.83
PRRT2	0.004497579	-2.69
PRRX1	6.35E-08	4.47
PSD	0.000115989	-3.30
PSD2	4.26E-11	-5.20
PTPN5	0.040760153	-2.22
PTPRO	0.021798893	-3.79
PTPRZ1	0.007242019	-2.76
RAB11FIP4	0.001959665	-2.61
RAB3A	5.32E-12	-5.54
RAB3B	0.006185163	-3.68
RAB3C	0.016752353	-2.36
RAB6B	0.000165693	-3.47
RACGAP1	0.061111711	-2.05
RADIL	0.050092741	-2.62
RAP1GAP	0.073287114	-2.26
RAPGEF5	3.79E-07	-6.01
RASD2	0.002144591	-2.96
RASGEF1A	0.00518523	-5.67
RASGEF1B	0.029744925	-2.94
RASGRF1	0.000983191	-5.51
RASGRP1	8.01E-08	-8.05
RASGRP2	0.000661167	-3.95
RASL10B	0.061380563	-2.08
RASSF4	0.024259042	1.84
RBFOX3	1.70E-05	-6.20
RCC2	0.094164925	1.63
RCN1	0.041222555	1.83
RCN3	0.003630156	2.39
RCOR2	0.000710639	-3.05
RECK	0.008590251	2.45
RELL2	0.028496092	-2.69
REM2	2.10E-05	-9.44
RERG	1.40E-10	6.42
RFX4	0.060272216	-1.70
RGS10	0.074352913	2.24
RGS17	0.087574304	-2.99
RGS7BP	0.000573434	-4.66
RGS8	5.36E-06	-14.61
RHBDL3	0.000214365	-2.92
RIMS1	0.000112905	-5.01
RIT2	0.077995105	-1.94
RND1	0.009754406	-3.99

Nature Neuroscience: doi:10.1038/nn.4532

RND2	0.010976423	-2.69
RNF152	0.040760153	-3.05
ROBO2	0.065861491	-2.00
RPH3A	0.050576525	-2.80
RPS6KL1	1.25E-08	-5.90
RSPH9	0.038137748	-3.53
RTN1	1.84E-06	-3.98
RUNDC3B	7.09E-07	-5.05
S100A4	0.000484567	6.51
S1PR1	0.014593437	-2.66
SAPCD2	0.015907556	-2.56
SCAMP5	0.0443503	-2.19
SCN1A	9.31E-06	-3.69
SCN2A	4.93E-07	-4.43
SCN3A	0.021598665	-2.14
SCN3B	0.000119026	-3.13
SCPEP1	0.004019005	2.17
SDC1	0.074660479	1.71
SELENBP1	0.00223656	2.43
SEMA3D	0.025926829	2.56
SEMA3F	0.097359548	1.76
SEMA4A	0.034745853	-3.27
SEMA6B	0.089842085	1.81
SERPINH1	0.008945957	2.68
SERTAD3	0.014745916	2.25
SERTM1	1.62E-07	6.11
SEZ6L	2.34E-12	-5.00
SFRP2	0.035789763	2.00
SGCD	0.000235438	11.35
SGIP1	0.007740785	-2.82
SGK223	0.088794472	-2.23
SGSM1	0.000381025	-2.98
SH3GL2	0.090892872	-1.79
SH3PXD2A	0.003047099	2.86
SHANK1	2.66E-05	-3.79
SHC1	0.080768256	1.67
SHC3	0.000463481	-3.90
SIX5	0.08623998	1.72
SKA2	0.087076367	-1.88
SKIDA1	0.020780085	-2.36
SLC10A4	0.03146761	-3.33
SLC12A5	0.000532293	-3.58
SLC15A2	0.002739031	2.93
SLC16A4	8.15E-06	4.50
SLC17A6	3.23E-15	-6.86
SLC17A7	0.016473488	-2.38
SLC1A2	3.13E-05	-3.93
SLC22A3	0.007992573	2.08
SLC24A2	0.019007684	5.56
SLC27A2	0.001195573	-13.43
SLC2A10	0.07900968	1.71
SLC2A3	0.000696427	-2.71
SLC43A1	0.058730866	2.60
SLC6A15	0.015131541	-3.27
SLC7A11	0.033256762	2.08
SLC7A14	3.78E-05	-4.32
SLC7A2	0.006411678	2.50
SLC8A1	0.000578882	-3.13
SLIT1	8.87E-06	-4.49
SLITRK1	1.13E-10	-5.96
SMAP2	0.040866033	-2.15
SNAP23	0.038879915	2.08
SNAP91	1.79E-12	-4.98
SNCA	0.019743561	-3.54
SNCB	4.57E-09	-5.98
SNTB2	0.098920341	1.81
SNX9	0.033985927	1.86
SOCS2	0.020164056	-2.39
SOSTDC1	0.000197221	3.37
SOX2	0.0108565	-2.56
SOX21	0.003342096	-2.42
SOX5	0.032392317	-2.21
SOX8	0.075232112	1.70
SPATS2L	0.001237168	2.79
SPSB4	0.006609018	-3.35
SPTBN4	0.008523499	-3.94
SREBF1	0.075474147	1.63
SSTR2	0.005575817	-2.98
ST18	5.09E-05	-2.46
STK3	0.077817883	2.02
STK32B	0.001794726	3.67
STK39	0.059159574	-2.08
STMN2	2.03E-09	-4.97
STMN4	1.08E-17	-7.44
STX1A	0.007726345	-2.81
STXBP1	7.47E-05	-3.31
STXBP5L	0.043166502	-1.91
SULT4A1	0.002533102	-3.04
SUMF1	0.036659671	1.90
SV2A	0.053682826	-2.09
SVIL	7.74E-06	3.98
SYBU	0.000301755	-2.95
SYN3	0.003530721	-2.84
SYNGR2	0.010329365	2.33
SYNGR3	1.25E-10	-5.52
SYT1	5.94E-06	-3.67
SYT3	0.003051398	-2.84
SYT5	1.38E-06	-5.36
SYT7	0.019877849	-2.16
TEAD2	0.012697126	2.12
TEKT2	0.067546159	-3.46
TGFB3	2.40E-06	3.74
TH	0.000980297	-13.61
THBS1	0.004020437	2.16
THSD4	0.050511603	-2.08
THSD7A	0.013379292	-2.69
TMEFF2	0.001167317	-4.16
TMEM100	0.014787056	1.82

Nature Neuroscience: doi:10.1038/nn.4532

TMEM170B	0.002447445	-2.36
TMEM39A	0.011918424	2.24
TMOD2	0.001735375	-2.65
TMTC1	3.55E-11	7.22
TNFAIP6	0.000264084	4.17
TNIK	0.080689227	-2.00
TNS3	0.042410222	1.73
TOP2A	0.082327583	-1.86
TOX	2.76E-05	-3.85
TP53	0.087076367	1.74
TPPP	1.62E-07	-4.06
TRAM2	0.000251705	2.89
TRIM2	0.018795399	-2.37
TRIM46	0.087357961	-2.42
TRIM67	2.32E-18	-5.76
TRIM9	0.021616902	-2.58
TRIP6	0.00445933	2.19
TRPS1	0.018739683	1.95
TRPV2	0.084657198	-5.09
TSPYL4	0.074107166	-1.97
TUBB6	0.033804754	1.84
UNC13A	3.42E-09	-4.67
UNC5A	1.31E-08	-6.23
VAMP2	0.004198136	-2.55
VAT1L	0.050214021	-2.48
VAV2	0.032706336	-2.22
VEPH1	0.010334734	-3.40
WASF1	0.043704124	-2.09
WDR17	0.006117981	-2.43
WIPI1	0.069534545	1.81
WNT5A	0.007459924	2.27
WNT7B	4.08E-18	-12.72
WWTR1	1.96E-05	3.38
XPR1	0.000887513	-3.09
YAP1	0.040393581	2.01
YPEL4	0.036887419	-2.66

ZCCHC24	0.003506095	2.34
ZNF536	0.038668336	-2.12
ZNF558	0.008184637	-3.88
ZNF608	0.065497212	-2.08
ZNF667	3.70E-05	9.48
ZSWIM5	6.88E-06	-3.60
AARD	0.050576525	-6.83
ABCA3	0.035431542	-2.17
ABCA8	0.000139798	2.88
ABCB1	1.13E-06	-8.69
ABCC3	0.062286455	-4.98
ABI3BP	0.0195545	1.94
ABRA	1.16E-05	78.63
ACBD7	0.001428797	-3.31
ACPL2	0.011881987	-2.52
ACTC1	4.98E-10	74.04
ADAMTS1	0.009372033	2.11
ADAMTS14	7.94E-10	6.29
ADAMTS17	5.92E-05	5.65
ADAMTS9	0.040262621	1.97
ADAP2	0.04374308	-5.76
ADCY7	0.036687615	-2.18
ADD2	6.35E-08	-6.36
ADM2	0.032313375	2.17
ADPRHL1	0.003427511	8.35
ADRB2	0.035007032	3.77
ADRBK2	0.092942757	-1.92
AFF3	0.099669827	-1.80
AGMO	0.026339597	7.08
AGR3	0.038916164	-101.33
AGT	0.096905986	1.60
AGXT	0.04374308	8.80
AHCY	0.002110749	2.51
AHR	0.020870555	1.95
AK1	0.047342986	1.81
AKAP12	0.002971482	-2.87

AKAP5	0.033102995	-2.77
AKAP6	0.038760505	-1.96
AKR1B1	0.036687615	1.84
AKR1C3	0.012449907	2.53
ALDH1B1	0.009126212	2.40
ALDH5A1	0.031704884	-2.04
AMIGO1	0.023524892	-2.60
AMN1	0.003126531	-3.05
AMOTL2	0.087076367	1.67
AMPD1	0.095240604	8.65
ANGPTL2	0.002431428	2.51
ANKRD29	0.005561956	4.21
ANKRD35	0.048680362	-6.06
ANKRD46	0.018957652	-2.33
ANKS1B	0.03973398	-2.82
ANO6	0.049397113	2.09
ANPEP	0.000662215	4.95
ANXA1	0.000368535	2.56
ANXA11	0.000481673	2.85
ANXA3	0.021616439	-13.81
AP3B1	0.021240266	2.01
AP3B2	6.48E-08	-4.95
APBA2	0.065497212	-2.13
APBB3	0.057836947	-2.41
APC2	0.000170621	-3.24
APLNR	0.079226702	3.32
AQP1	5.14E-05	3.57
ARAP3	0.092473971	-2.38
ARG1	0.050092741	-7.61
ARHGAP10	0.002673738	5.38
ARHGAP21	0.001908863	-2.88
ARHGAP24	0.000249084	3.36
ARHGAP28	0.056112204	2.62
ARHGAP33	7.37E-07	-4.18
ARHGAP8	0.005947486	-5.10
ARHGEF10L	0.084442911	-2.19

Nature Neuroscience: doi:10.1038/nn.4532

ARHGEF2	0.007524571	2.21
ARHGEF4	0.096995131	-1.96
ARL4C	0.048826316	-2.24
ARNT2	0.040854324	-1.98
ARRB2	0.061304751	-2.12
ARSJ	0.000431205	3.86
ASGR1	0.064890225	-3.10
ASIC4	0.001222007	-3.47
ASS1	0.033922836	1.73
ASTN1	0.097795043	-1.72
ATAT1	0.001339306	-2.70
ATCAY	6.33E-05	-3.30
ATG9B	6.35E-05	-15.04
ATOH7	0.008922508	-8.97
ATP13A2	0.09920535	-1.99
ATP6V0A1	0.080110588	-1.96
ATP8B3	0.003551215	-4.90
ATRNL1	0.002375382	-2.59
ATXN8OS	0.02590021	-9.33
AVP	0.009664283	-101.33
AZGP1	0.003927563	-24.09
B3GALT2	0.018738455	-2.90
B3GAT1	0.001049373	-2.63
B3GNT4	0.006462217	-6.50
B4GALNT3	0.001827511	2.66
B4GALT1	1.49E-06	3.73
BAG2	0.002956507	3.46
BAIAP2L1	0.001989562	4.07
BAIAP3	0.039701501	-2.06
BARX1	0.000673931	4.24
BASP1	0.060272216	-2.41
BCL11A	0.08413548	-3.14
BDKRB2	2.39E-08	5.59
BHLHE23	0.036327258	-7.72
BHLHE40	0.001624423	-2.84
BHMT	0.006439415	-11.71

BIRC7	0.052660411	-10.45
BLCAP	0.032548511	2.18
BMP1	0.002751397	2.37
BMP5	0.005606598	2.56
BNC1	0.023464383	6.82
BNIP3	1.97E-07	-3.96
BPIFB4	0.089450151	16.88
BRSK1	0.00053606	-3.16
BRSK2	0.005397448	-2.50
BSN	4.59E-12	-4.99
BTNL9	0.00143586	-5.80
BVES	0.002206614	2.62
BZRAP1	2.54E-05	-3.76
C10orf10	0.002804654	4.19
C10orf82	0.018705371	-10.76
C11orf35	1.17E-05	-6.16
C12orf42	0.001090023	28.68
C12orf49	0.04541411	-1.94
C15orf59	0.068851012	-2.38
C17orf102	0.019657283	-4.79
C1orf21	0.016797455	-2.27
C1orf61	0.00047423	-3.09
C1orf94	0.061428385	-9.37
C1QL4	0.000176813	-3.32
C20orf112	3.12E-05	-3.45
C2orf80	0.002906484	-3.66
C3orf52	0.043774909	3.39
C4orf17	0.074950938	9.67
C5orf30	0.010629284	-2.45
C5orf38	0.021895364	-3.69
C5orf64	0.00126146	-13.60
C6orf1	0.056207452	-2.66
C6orf106	0.065384426	1.82
C6orf48	0.025590325	1.92
C9orf135	0.07237579	-8.07
CA12	0.000926006	-3.10

CA9	2.59E-05	-5.98
CABP1	0.07304897	-4.14
CACNA1I	0.036687615	-2.76
CACNA2D4	0.065325558	5.55
CADM4	0.096466675	-2.09
CAMK2N2	8.68E-06	-3.95
CAMSAP2	0.075232112	-1.94
CARNS1	0.00173417	5.06
CASP4	0.060194627	4.39
CASP7	0.037152514	1.92
CASZ1	0.005317884	4.11
CATSPERG	0.070190562	-2.88
CCDC113	0.071589305	-2.13
CCDC136	0.007726345	-2.62
CCDC3	0.000315561	3.33
CCDC33	0.024249962	-6.86
CCDC69	0.000213043	3.63
CCDC8	0.001479499	2.46
CCDC88B	0.006588591	-4.89
CCDC88C	0.003831956	-2.38
CCL11	0.08413548	416.25
CCL20	0.007621317	-32.72
CCNA1	0.013080719	-5.92
CCNG1	0.084291393	1.69
CCNG2	0.009896302	2.27
CCSAP	0.025851322	-2.27
CD109	0.078546589	1.86
CD164	0.021404556	2.14
CD2	0.005283972	25.09
CD200	7.74E-06	-3.62
CD248	4.73E-12	6.26
CD34	0.000194267	5.78
CD44	0.003880114	2.03
CD8A	0.058082733	-4.58
CDC42BPG	0.014120152	-4.81
CDH2	0.007524571	-2.43

Nature Neuroscience: doi:10.1038/nn.4532

CDHR1	0.040637196	-2.85
CDHR2	0.010479103	-5.86
CDHR3	0.016969685	-2.87
CDKN1C	1.32E-06	5.66
CDKN2D	6.48E-07	-4.49
CEBPA	0.000329685	3.46
CECR6	0.001393386	-3.21
CELF3	1.15E-17	-6.72
CELF4	1.61E-12	-6.14
CELF5	9.05E-06	-3.93
CELF6	0.009611063	-3.16
CELSR2	0.007726345	-2.29
CELSR3	0.006647446	-2.48
CENPV	0.00550658	-3.15
CERCAM	0.027703153	1.88
CFHR3	0.019394119	82.25
CFL2	0.087807028	1.76
CHAT	0.008939553	-7.32
CHCHD6	0.095985357	-2.46
CHML	0.020312561	-2.36
CHMP3	0.083673745	1.65
CHRD	0.003943353	2.29
CHRNA2	1.10E-18	-31.90
CHRNA5	0.093576045	-2.44
CHRNA6	0.003495279	-20.21
CHRNB2	1.62E-06	-3.97
CHRNB4	3.00E-05	-6.35
CHST8	0.00309472	-5.82
CHSY1	0.025556971	2.02
CILP2	0.03286606	-2.44
CKAP4	0.07716856	1.81
CLASP2	0.001975993	-2.71
CLDN19	0.037371683	-23.27
CLDN3	0.000294016	-19.04
CLEC1A	0.029330483	6.83
CLEC3B	0.09094893	6.56

CMIP	0.040656663	-2.06
CMKLR1	5.81E-05	3.21
CMTM7	0.074168801	2.84
CNGA3	0.054719489	-2.45
COL12A1	0.000221499	3.08
COL14A1	8.98E-06	6.67
COL16A1	3.67E-10	4.73
COL21A1	3.28E-10	6.48
COL23A1	0.022465688	1.89
COL24A1	0.000201401	3.21
COL26A1	0.075687379	1.85
COL5A1	0.015410964	3.25
COL5A2	0.09983487	2.04
COL5A3	3.03E-06	3.92
COL6A3	0.00179205	5.14
COLEC12	0.001070009	2.36
COLGALT2	1.93E-05	3.93
CORO2B	0.00349003	-2.71
CORO7	0.02193309	1.93
COTL1	0.023984908	-2.23
CPLX3	0.08503098	-4.71
CPNE7	0.084291393	-3.79
CPNE9	0.003195994	-8.20
CPVL	0.002611392	2.75
CPZ	0.035565759	3.24
CRB2	0.081563961	-1.66
CREB3L1	0.001636752	2.52
CREB3L2	0.025050638	1.97
CREB5	0.050706819	-1.88
CREG2	0.006185163	-3.37
CRHBP	0.038772185	-5.82
CRHR2	0.002138403	-8.36
CRISPLD2	1.48E-07	4.23
CRTAP	0.024881085	2.08
CSPG4	0.000482117	2.74
CTDSPL	0.019430795	2.42

CTNNA2	0.007072808	-2.24
CTNND2	1.57E-05	-3.50
CTSK	8.52E-07	4.02
CUBN	0.002189761	-4.35
CXCL12	0.002699786	7.97
CXXC11	4.83E-08	-46.35
CXXC4	0.023374608	-2.65
CYB561A3	0.052660411	2.14
CYB5R1	1.23E-06	3.63
CYP1B1	5.11E-05	3.33
CYP2S1	0.023943968	-4.30
CYTIP	0.030123106	12.11
DAAM1	0.001471119	-2.71
DACT2	0.073656698	-3.52
DDC	0.035850899	-3.50
DDR2	0.001593539	2.89
DEFB1	0.029366604	-101.33
DENND1C	0.011219084	-3.88
DEPTOR	0.049066718	1.84
DGKI	0.021598665	-2.47
DHRS13	0.040413867	-2.57
DHRS2	0.061513539	-3.98
DIRAS3	0.003104966	2.22
DKK2	0.002120238	4.29
DLG1	0.086013718	1.72
DLGAP3	0.000983191	-4.40
DLL4	0.062733793	-3.93
DLX3	0.036915053	9.48
DMPK	6.72E-05	3.00
DNAJC21	0.045409319	2.00
DNAJC22	0.089294738	-3.60
DNMT3B	0.005244172	-3.29
DPT	9.52E-05	3.60
DPY19L2P2	0.053054321	-4.14
DPYD	0.054285586	1.98
DPYSL4	0.086803056	-2.01

Nature Neuroscience: doi:10.1038/nn.4532

DPYSL5	0.013498837	-2.78
DQX1	0.004045201	-13.71
DRD4	0.057305181	-4.61
DSE	0.000275742	3.02
DTX3	0.078706241	-2.12
DTX4	0.00118962	-2.61
DUOX1	0.026467147	-3.21
DUOX2	1.36E-05	-9.83
DUSP1	0.007685373	2.29
DUSP13	2.34E-05	27.21
DUSP5	0.025998147	-3.08
DUSP8	6.45E-11	-5.06
ECM2	0.008801076	3.92
EDN1	0.000678613	-19.26
EDNRA	1.66E-11	6.06
EEF1D	0.045179553	1.70
EFEMP1	0.000641541	2.37
EFNB2	0.000652306	-3.07
EFR3B	0.000438654	-2.61
EGFL7	0.094717194	1.53
EHD2	0.012609085	2.02
EIF3E	0.037062674	2.00
EIF4E1B	0.032548511	-7.75
ELAVL2	0.00041246	-2.87
ELAVL3	1.78E-16	-7.14
ELMSAN1	0.054350814	1.86
ELN	0.001212065	2.74
ELOVL1	0.048219253	1.94
ELOVL2	0.005411215	-2.46
EMILIN1	0.00978521	1.97
EMILIN2	0.002185448	3.31
EMILIN3	0.007915656	2.63
EMP3	0.073218117	1.63
EMX2OS	0.026508943	2.17
EN1	0.008922508	-3.28
ENG	0.000322629	3.75
ENPP1	0.000427796	4.03
ENPP2	0.03481198	2.09
ENPP6	5.21E-05	6.83
EPAS1	0.055789952	-2.57
EPHA10	0.058168121	-5.39
EPS8L1	0.002563121	-5.89
EPS8L2	0.005623458	-4.74
ERBB3	0.079226702	4.11
ERO1L	0.023460653	-2.22
ESRRA	0.068317651	1.98
ESYT1	0.007726345	2.24
ESYT3	0.068880696	2.29
EVC	0.054476839	1.84
EVL	0.001599798	-2.81
EYA1	0.005669618	3.40
F11R	0.027970741	-2.26
F2RL1	0.098592244	-2.40
F2RL2	8.93E-05	3.35
FABP6	0.00094343	-28.81
FADS6	0.001417857	-9.65
FAM101B	0.015074906	2.33
FAM109B	0.008560903	-15.11
FAM114A1	0.020654393	2.09
FAM117B	0.000384104	-2.96
FAM120A	0.018478926	2.07
FAM126B	0.018957652	-2.39
FAM129A	0.002872813	2.34
FAM131B	6.83E-05	-3.24
FAM163B	0.008751485	-7.07
FAM219A	0.000292927	-3.17
FAM26E	0.017013079	3.58
FAM43A	0.035601503	1.83
FAS	0.000328907	3.11
FAXC	3.98E-07	-5.41
FBXL16	0.001339306	-2.94
FBXO10	0.001220812	2.74
FBXO21	0.074255908	-1.97
FBXO40	0.007945721	28.63
FBXO41	3.03E-05	-3.40
FBXW4	0.053682826	2.33
FCGRT	0.027206467	1.85
FCHO1	0.009525841	-2.80
FDCSP	0.030179788	-12.00
FGF10	0.005108568	3.74
FGF17	0.072206562	-4.28
FGF19	0.001248933	-10.77
FGF7	8.63E-09	8.72
FGFBP1	0.036902005	9.32
FGFR4	0.000203161	3.44
FIBCD1	2.68E-05	-7.13
FKBP7	0.000604137	2.69
FLNC	3.10E-05	4.73
FLRT1	0.03286606	-2.43
FLVCR2	0.001518322	4.54
FMN2	0.070115801	-1.69
FN3K	0.07599492	-2.56
FNBP1L	0.038846536	-2.28
FOLH1	0.068261035	-6.76
FOXC1	0.049160858	2.28
FOXF1	0.084779461	2.63
FOXK1	0.075687379	-1.73
FRMD4A	0.038301741	-2.11
FRMD5	0.003451915	-4.30
FRZB	0.000759082	2.71
FSHR	0.004567331	45.67
FUT3	0.00035136	-13.84
FUT5	0.004146977	-12.34
FXYD3	0.002227098	-101.33
FYCO1	2.43E-05	3.23
FZD10	0.061218153	2.45
FZD3	0.007726345	-2.13
FZD4	0.026774219	2.03

Nature Neuroscience: doi:10.1038/nn.4532

FZD5	0.086238313	-2.52
GABRD	0.074484467	-4.78
GAD2	0.011005476	-2.83
GADL1	0.038760505	11.79
GALNS	0.046791324	1.94
GALNT12	0.07599492	-3.20
GALNT9	0.011132686	-4.05
GALP	0.004555918	-101.33
GAP43	0.004976518	-3.24
GAS5	0.026455557	2.03
GBP5	0.014542826	15.53
GCK	0.070640066	-3.47
GDAP1L1	5.05E-07	-4.27
GDF6	0.008356201	3.53
GGTA1P	4.06E-09	15.74
GHR	0.081563961	2.79
GIT1	0.099621849	-1.98
GJA5	0.011881987	12.88
GLB1L2	0.01572579	-2.47
GLS2	0.004979682	-4.39
GLT8D2	4.27E-11	6.15
GLTPD2	0.06321316	-4.77
GLYATL1	0.034852601	-5.47
GMPPA	0.08338071	1.78
GNG13	0.057572474	-6.93
GNRH1	0.055731677	-9.23
GOLT1A	0.028833877	-9.35
GPC2	0.004025222	-2.50
GPD1L	0.025468157	1.98
GPM6A	0.005107938	-3.08
GPNMB	0.00060291	2.47
GPR124	9.08E-06	3.48
GPR126	0.028012163	-2.66
GPR133	4.84E-05	6.59
GPR137C	2.50E-06	-4.23
GPR141	0.072686545	24.96
GPR160	0.026412111	-7.19
GPR56	7.91E-05	-3.13
GPR61	0.057753999	-3.51
GPRC5C	0.057943328	1.75
GPRIN1	1.62E-07	-4.00
GPRIN2	0.040393581	-3.72
GPRIN3	3.26E-05	-4.14
GRAP	0.017646008	-9.27
GRB7	0.035662301	-9.53
GRIK5	0.021399868	-2.23
GRIN2C	0.013000193	-6.99
GRIN2D	8.28E-09	-4.25
GRIP1	0.038473349	-2.48
GRIP2	0.007500416	-3.47
GSE1	0.069312653	-2.15
GUCA1A	1.51E-05	-11.27
GXYLT2	0.002284913	2.46
GYG1	0.004432938	2.16
H6PD	0.007104834	2.24
HAPLN2	0.012565899	-5.07
HAPLN3	0.046286906	2.02
HAR1A	0.00050953	-7.02
HAS1	0.003013545	-10.85
HDAC5	0.003387947	-2.71
HDAC9	0.003767484	-4.37
HERC1	0.099621849	-1.89
HEY2	0.014085633	2.78
HHATL	0.016070334	13.77
HHIPL1	0.043288216	-4.87
HID1	0.001014717	-2.82
HIF1AN	0.067208744	1.85
HILPDA	2.02E-07	-5.05
HIPK3	2.66E-05	3.47
HIPK4	0.000156085	16.58
HIST1H2BK	0.008993051	3.40
HKDC1	0.008758467	-5.30
HLA-DRB1	0.099661362	4.12
HLX	0.000352039	5.78
HMCN1	0.002152773	2.41
HMGA1	0.075211712	-2.02
HMGCR	0.089022586	-1.90
HMGCS1	0.047596228	-2.08
HMP19	8.56E-16	-7.92
HNF4A	0.008590251	-101.33
HOMER3	0.097097556	1.63
HOXA10	0.020238499	2.12
HOXA11	2.24E-06	4.54
HOXA11-AS	0.021671583	4.63
HOXA13	0.012011559	8.26
HOXB13	0.000305335	4.89
HOXD13	0.007194909	4.67
HPX	0.002281222	-8.25
HSD11B1	0.055731677	37.88
HSDL1	0.021240266	-2.17
HSF4	0.064835234	-2.58
HSPA12B	0.072746801	2.54
HSPB1	0.004249474	2.27
HSPG2	0.062527336	1.79
HTR1E	0.024097792	-6.24
ICMT	0.011828489	2.09
ICOSLG	0.091722393	2.34
ID3	1.11E-10	5.29
IFRD2	0.013516808	2.18
IGDCC4	0.097795043	1.64
IGF2R	0.010558578	2.59
IGFBP4	0.071687643	6.37
IGFBPL1	9.08E-05	-3.77
IGFL2	0.057836947	-23.33
IGSF10	0.098454251	1.96
IGSF9	3.17E-05	-4.19
IKZF2	0.034820751	-2.48
IL11	0.014901682	-4.57

Nature Neuroscience: doi:10.1038/nn.4532

IL11RA	0.034785715	1.92
IL1R1	2.25E-05	3.13
IL4R	0.023592653	5.19
IL6	0.064574859	-5.80
IL6R	0.092187142	3.06
IMPA2	0.002284913	2.71
IMPDH2	0.049140498	1.89
INPP5D	0.061380563	-4.56
INSL5	0.007915656	-6.72
INSM2	0.000715893	-27.43
IP6K3	0.000247862	9.33
IPO4	0.095613198	1.73
IPW	0.099730956	1.63
IQSEC3	6.86E-05	-6.56
IRS2	0.030394706	-2.15
IRX2	0.013746725	-3.21
IRX6	0.062162922	4.52
ITGA11	0.005358305	2.08
ITGA5	0.00195641	2.40
ITGA8	3.00E-06	8.20
ITGA9	0.072418678	2.57
ITGB1	0.038568908	1.94
ITGB3	0.099536982	3.18
ITPR1	0.003352648	2.35
ITPRIPL2	0.000586276	2.92
JAK3	0.041438489	-2.93
JARID2	0.012530825	-2.24
JDP2	0.000404662	2.66
JPH2	0.004512698	13.23
KANK2	4.28E-05	2.93
KANK4	7.49E-07	4.55
KAZALD1	0.013747135	3.02
KBTBD11	0.002077401	-2.66
KBTBD6	0.067669586	-1.97
KCNA5	0.07667158	-4.90
KCNC1	0.025970616	-6.71
KCNH6	0.000396154	-24.41
KCNH8	0.007678249	-3.32
KCNJ3	0.097359548	-4.23
KCNJ4	0.030527788	-2.47
KCNJ5	0.001612959	-15.02
KCNJ9	2.03E-10	-11.33
KCNK12	0.020654393	-3.31
KCNK15	0.001195573	5.04
KCNK3	0.0195545	-2.20
KCNS3	2.70E-05	7.15
KCTD12	0.027703153	1.95
KCTD7	0.060486212	-2.07
KDELC2	0.000708488	2.51
KERA	0.032074851	5.71
KHDC3L	0.021861371	-17.74
KIAA0408	2.37E-05	-3.41
KIAA0895	0.064944971	-2.11
KIAA0895L	0.025111792	-2.44
KIAA1147	0.00588986	-2.31
KIAA1467	0.002766844	-2.55
KIAA1549L	0.014123272	-2.35
KIAA1644	0.03973398	-2.21
KIAA1804	0.008162529	-3.91
KIAA1958	0.018578549	-2.15
KIF16B	0.026669401	2.35
KIF1C	0.028278038	1.93
KIF21A	4.12E-05	-2.94
KIF21B	1.15E-11	-5.55
KIF3A	0.004875762	-2.44
KIF3C	1.36E-05	-3.74
KISS1R	5.56E-06	-8.62
KLF2	0.017845142	3.33
KLF4	2.33E-16	9.21
KLF7	0.001959665	-3.72
KLHDC8A	0.008776178	-2.36
KLHL14	0.021528919	-2.90
KLHL21	0.015740817	2.05
KLHL30	0.000345588	12.06
KLHL32	0.055511122	-2.52
KLHL38	0.009460132	45.15
KLHL41	1.04E-19	55.19
KLK6	0.052660411	-101.33
KRT80	0.069383005	6.98
KRTAP5-1	0.001528053	-12.09
KRTAP5-2	0.00204334	-5.85
KRTAP5-AS1	1.13E-05	-6.78
KSR2	8.19E-06	-5.77
L1TD1	0.021614863	11.38
LAMA2	1.27E-11	6.68
LAMB1	0.016499913	2.25
LAMB2P1	0.030280891	-3.83
LAMC1	0.005908199	2.78
LAMP5	0.00341996	-2.49
LAPTM4A	0.09722142	1.78
LBH	0.020626678	-2.26
LCOR	0.032620878	-2.53
LCORL	0.098782608	-1.96
LDB3	9.42E-13	78.47
LDLRAD2	0.089640893	1.62
LDLRAP1	0.017494596	2.50
LEPRE1	0.000269918	2.82
LEPREL1	0.00133784	2.86
LEPREL2	0.002582594	2.21
LGR5	0.050706819	3.03
LHFPL2	2.26E-06	3.46
LHX1	7.15E-06	-11.48
LHX8	0.003086467	8.40
LIFR	0.043447986	-1.82
LINC00930	0.03797565	9.57
LINC00950	0.00298029	-2.59
LINGO3	7.14E-07	-39.85
LMNA	1.76E-08	4.72

Nature Neuroscience: doi:10.1038/nn.4532

LMO7	0.075335846	2.02
LMTK2	0.053889457	-1.95
LOC339240	0.014335506	24.90
LOC441204	0.025459532	-3.10
LONRF2	0.001518591	-2.69
LPAR2	0.007973845	-2.82
LRFN1	0.095825577	-2.10
LRP2BP	0.017120716	-3.27
LRP8	1.85E-05	-4.32
LRRC14B	0.02193309	13.39
LRRC16B	1.38E-06	-5.09
LRRC2	0.044532245	7.50
LRRC20	0.061304751	-2.00
LRRC26	0.037726825	-5.25
LRRC3	0.072418678	-2.23
LRRC39	2.20E-05	7.83
LRRK1	0.009412079	3.99
LRRN1	0.002209679	2.81
LRRN4CL	2.97E-06	4.47
LRTM1	0.028496092	15.60
LSP1	0.003996178	8.63
LZTS3	0.002118836	-2.95
MADCAM1	0.089905942	-4.82
MAFA	0.065303478	5.18
MAFF	0.063292547	-2.77
MAGEL2	0.041666512	-2.07
MAGI1	0.037371683	-2.18
MAGI3	0.023984628	-2.46
MALL	0.000426876	-19.86
MAMSTR	0.011499862	4.21
MAN2B1	0.094717194	1.66
MAP1B	0.021528919	-3.25
MAP2	0.013422993	-2.79
MAP3K10	0.028072421	-2.37
MAP6	0.001552102	-3.20
MAP7	0.061823197	-2.43

MAPK11	0.010374344	-2.68
MAPK8IP2	0.001039876	-2.93
MAPT	9.08E-05	-3.83
MARK1	1.57E-05	-3.62
MAST1	2.74E-07	-4.07
MAT1A	0.015209499	-6.84
MATN2	0.01508391	1.83
MCF2L2	0.02042631	-3.15
MCOLN3	0.013629831	6.42
MEIS1	0.01618628	-2.34
MET	0.030451161	3.57
MFAP5	1.77E-06	26.27
MFSD4	0.006969613	-3.77
MGAT5	0.018457351	-1.90
MGAT5B	0.007436033	-2.49
MGP	5.65E-07	3.88
MIAT	0.000870525	-3.48
MICAL3	0.074109222	-2.23
MINA	0.000165778	3.08
MKRN3	0.000109246	-6.77
MLLT11	0.048162535	-2.31
MLLT4	0.002712592	-2.48
MLXIPL	0.000301417	-5.24
MMP15	7.10E-05	-3.17
MMP2	6.63E-05	4.32
MOCOS	0.00384265	4.03
MORN4	0.0195545	-2.42
MPP2	0.016988094	-2.23
MPPED2	0.065020092	-2.06
MRAP2	0.021058041	2.39
MS4A6A	0.033798325	-101.33
MSC	2.92E-12	9.92
MSR1	0.075211712	26.16
MSRB3	5.51E-06	4.09
MSTN	0.014335506	2.53
MSX1	8.40E-07	3.90

MT1A	0.0901614	-17.52
MT1E	0.022171624	-3.80
MT1F	0.024881085	-3.55
MT1X	0.017540088	-3.37
MT2A	0.001077321	-4.35
MTG1	0.056720061	2.17
MTHFD2	0.078706241	1.84
MTMR4	0.066889075	-1.95
MTMR9	0.086620607	-1.88
MTTP	0.003455435	-3.65
MUSK	1.32E-12	29.68
MUSTN1	0.000947588	9.08
MVP	0.044133948	1.75
MXD1	0.008451978	-2.91
MYADM	0.057277493	1.81
MYCBP	0.00614038	3.13
MYCN	1.53E-05	-4.42
MYF5	0.00837844	15.20
MYF6	1.02E-12	68.89
MYH2	0.000438654	62.00
MYH3	2.21E-07	56.46
MYL12A	0.000138091	2.85
MYL7	0.000381025	-101.33
MYLIP	0.003492136	2.46
MYLK2	0.0002094	11.85
MYO1C	0.001190231	2.53
MYO5A	4.28E-05	-3.27
MYOF	0.007149397	2.03
NCKAP5	0.094717194	-2.39
NCOA7	0.035798857	2.11
NEBL	0.060194627	-1.99
NECAB3	0.005042355	2.30
NECAP1	0.025233688	-2.22
NEFL	0.000191632	-3.64
NEK9	0.00088215	2.68
NELL2	1.10E-05	-3.70

Nature Neuroscience: doi:10.1038/nn.4532

NETO2	0.015594906	-2.39
NEU4	0.02631817	7.58
NID1	0.000121019	3.14
NIM1	0.081363835	-2.68
NIPAL4	0.040721212	-5.73
NKAIN1	3.23E-10	-4.75
NKAIN2	0.002611304	-5.72
NLK	0.010561467	-2.30
NMRK2	8.86E-06	13.06
NMU	0.057647642	-4.92
NNMT	1.08E-07	3.81
NOG	0.062053072	2.58
NOS1AP	0.095628367	-2.62
NOS3	0.000165778	-16.59
NOTUM	0.088233235	2.99
NOVA2	0.000345588	-3.54
NPC1	0.020803948	2.08
NPTX1	0.008758467	-2.53
NPTX2	0.033985927	2.06
NPTXR	0.000917291	-3.38
NPVF	0.005953704	-13.87
NPY6R	0.050576525	11.65
NQO1	5.30E-06	3.40
NR1H4	0.003418922	-19.62
NREP	0.000340004	-3.61
NUAK1	0.055765321	-2.07
NXPH3	0.000746929	-4.10
NYAP1	2.37E-06	-4.20
OAF	0.099202684	1.56
OBSCN	0.095240604	1.72
OLFML1	3.29E-18	12.41
OLFML3	3.60E-11	5.02
ONECUT1	0.031352986	-7.95
ONECUT2	0.000278998	-3.53
ORM1	0.011191014	-101.33
OSR2	0.000560298	6.12
OSTC	0.000511814	2.59
OXTR	0.090450209	2.69
P2RX3	0.00144673	-6.41
P4HA2	4.98E-07	3.68
PABPC4	0.024731847	2.08
PACSIN3	0.002431428	2.46
PAFAH1B3	0.041410544	-2.29
PAH	0.000924654	-17.91
PAIP2B	0.000741514	-3.08
PALM2	0.024805783	1.98
PALMD	5.95E-07	4.71
PAQR5	9.86E-05	-7.24
PARD6B	0.091040116	-2.24
PARP9	0.011499862	2.10
PASK	0.049210128	-2.42
PAX5	0.000108431	-7.20
PAX7	0.052163677	5.89
PAX9	0.003367512	15.00
PBX3	0.000169247	-3.21
PCCA	0.059194577	1.98
PCDH18	0.036902005	2.01
PCDHB1	9.61E-05	416.25
PCSK1	0.00712324	2.31
PCSK6	0.058730866	-3.49
PDGFB	6.77E-06	-6.58
PDGFD	2.90E-05	3.29
PDIA2	7.79E-08	-8.94
PDIK1L	0.013006217	-2.47
PDLIM3	0.004061226	2.64
PDYN	2.22E-15	-31.60
PDZD7	0.001397186	-5.22
PEAR1	0.089507124	2.71
PEX5L	0.036687615	-4.00
PFKFB4	0.000292927	-3.73
PFKM	0.064211665	2.05
PGA5	0.000479653	74.08
PGAP1	0.061111711	-1.92
PGF	0.001141494	2.90
PGM2L1	5.77E-05	-2.99
PGM5	4.17E-08	5.10
PHLPP1	0.050388561	-1.86
PHYHD1	0.02437582	6.99
PIK3C2B	0.089640893	-1.90
PITHD1	0.067580204	-2.15
PITPNC1	0.014946468	-2.56
PITPNM3	0.032710227	-2.24
PITX2	9.47E-15	11.18
PKLR	0.041666512	-3.60
PLAC9	0.01567956	4.95
PLAGL1	0.001220812	2.59
PLAT	0.054476839	-2.41
PLAU	0.013963673	2.52
PLCD4	0.001042472	3.40
PLCH2	3.98E-06	-4.87
PLEK2	0.022434455	-13.23
PLEKHG3	0.094679406	1.93
PLEKHG4B	0.043495663	1.80
PLIN2	0.033941931	-2.79
PLSCR3	0.0620129	1.78
PLSCR4	0.010479103	1.92
PNMAL2	0.081832922	-2.44
PNPLA3	0.060049557	-2.58
PODXL2	3.96E-07	-4.56
POPDC3	0.002378153	6.50
POU2F2	6.35E-08	-7.35
POU3F1	0.007034544	-4.99
POU4F2	4.30E-09	-19.11
POU6F1	0.015578232	-2.58
PPM1E	0.000795295	-2.56
PPM1F	0.050388561	1.77
PPM1J	0.076374666	-2.66
PPP1CA	0.098342246	1.64

Nature Neuroscience: doi:10.1038/nn.4532

PPP1R13L	0.099424201	-2.41
PPP1R27	2.02E-10	-5.95
PPP1R3A	2.07E-05	46.22
PRELP	0.065461477	1.78
PREX2	0.074660479	-2.95
PRG2	0.002497204	-2.69
PRKAG3	0.071400234	14.44
PRKCG	0.000744906	-3.56
PRKG1	0.071687643	2.32
PRLR	0.01241092	3.27
PRND	0.002665696	5.05
PROCR	0.094050202	1.82
PRPH	0.000104146	-3.64
PRR5-ARHGAP8	0.020695279	-4.04
PRRX2	0.000764393	3.78
PRTFDC1	0.001549276	-4.34
PTCHD2	0.003232682	-2.80
PTGER4	7.80E-11	14.10
PTGFR	4.89E-07	3.93
PTGS2	0.095854241	3.16
PTH2	0.051439416	-6.80
PTK7	0.036360676	2.01
PTPRF	0.065861491	-2.12
PTPRH	0.001115694	-4.71
PTPRJ	0.06814957	-2.82
PTPRN2	6.68E-11	-4.78
PTPRS	0.036007515	-2.44
PTRF	0.000641541	2.65
PXDN	0.01538077	2.24
PXK	0.033955942	1.93
PXN	0.043664977	1.79
PYCR1	0.008523733	2.15
PYDC1	0.016326649	-23.13
PYGM	8.83E-06	7.61
QPCT	0.046514039	-3.08
QPRT	0.080689227	1.68
RAB26	0.001651175	-5.46
RAB39A	0.061823197	-2.78
RAB3IP	0.027703153	-2.37
RALGPS1	8.62E-06	-3.42
RALGPS2	0.07769864	1.86
RALYL	0.003098002	-3.62
RARA	0.054476839	1.78
RARG	0.020432704	1.96
RASAL1	0.01612115	-3.70
RASD1	0.033565405	-3.34
RASSF3	0.001255318	3.93
RASSF7	5.95E-05	-4.73
RBCK1	0.015483389	1.93
RBM24	0.027189536	5.96
RBM47	0.06001616	-3.13
RBP1	0.024583218	-2.24
RFK	0.061467436	-1.99
RFPL1	0.020164056	-3.54
RFPL1S	5.77E-05	-3.86
RFPL2	0.082801034	-5.05
RFX3	0.00938772	-2.43
RIC3	0.000635936	-2.86
RIMKLA	0.040393581	-2.09
RIMS2	0.009197331	-3.65
RIN3	0.009895319	2.80
RIPPLY2	0.071687643	-11.47
RNASE1	0.027823053	-44.00
RNF125	0.021539339	6.93
RNF141	0.020756078	-2.13
RNF144B	0.092942757	3.95
RNF165	4.19E-06	-4.02
RNF186	0.03241566	-13.93
RNFT2	0.016431944	-2.70
ROR2	0.000191895	2.76
RPE65	0.021197039	-3.38
RPL10A	0.082801034	1.70
RPL12	0.017902873	1.93
RPL13A	0.050817522	1.97
RPL22L1	0.027033644	2.33
RPL28	0.085610119	1.74
RPL31	0.083790496	1.65
RPL35	0.063617698	1.68
RPLP0	0.065478655	2.07
RPP25	0.035007032	-2.53
RPS12	0.026467147	2.00
RPS9	0.092489062	1.56
RPSA	0.068154067	1.72
RRBP1	0.018592846	1.95
RREB1	0.02056285	2.14
RSBN1	0.074279337	-1.93
RSPO1	0.010565403	3.20
RTN2	0.020465933	2.16
RTN3	0.021616902	-2.21
RUFY3	0.09248978	-1.98
RUNDC3A	5.77E-06	-3.94
RUNX1	0.03797565	4.79
RUSC2	0.045960996	-2.18
S100A11	0.000445317	2.47
S100A8	0.001552683	-52.53
S1PR2	0.007463967	2.92
S1PR3	0.050802665	1.77
SAMD10	0.020397988	-2.94
SAMD11	0.040475648	1.78
SAMD14	0.07237579	-2.21
SAMD9L	0.034392901	2.01
SBK1	3.47E-07	-4.33
SCD5	0.082112956	-1.98
SCG3	1.55E-06	-3.74
SCGB3A1	0.030025075	-101.33
SCN4A	0.070692609	3.78
SCN8A	0.033922836	-2.42

Nature Neuroscience: doi:10.1038/nn.4532

SCNN1A	0.036687615	-10.82
SCOC	0.082801034	-1.95
SCRT1	3.28E-10	-7.29
SCRT2	3.41E-17	-12.51
SDC2	0.040182054	1.96
SDCBP2	0.095628367	-3.67
SEC11A	0.011977226	2.04
SEC11C	0.023389631	-2.42
SEC14L5	0.016752353	-5.17
SEC24D	0.011658994	2.14
SEMA3G	0.000105626	8.08
SEMA4G	0.024524598	-2.28
SEMA7A	0.001941577	-3.40
SERPINB9	0.020164056	-4.54
SERPINF1	1.09E-06	4.16
SESTD1	0.005922035	-2.48
SETD7	0.000191895	3.19
SFN	0.010859782	-17.49
SFXN1	0.099730956	-1.88
SGMS2	0.078952851	2.70
SH2D3C	1.98E-07	-5.20
SH2D5	0.026774219	-2.83
SH2D7	0.03124747	-4.00
SH3D19	0.00503862	2.44
SH3RF2	0.027941486	5.94
SHQ1	0.076107778	1.93
SIM1	0.082211316	3.83
SIPA1L3	0.084287019	-2.01
SIRPA	0.046556136	1.70
SIX1	1.16E-12	7.07
SIX2	7.55E-19	8.90
SIX4	0.001893998	3.29
SKOR1	0.002550213	-5.33
SLAIN1	0.003492136	-2.64
SLC12A8	0.001362411	-4.93
SLC16A14	0.00991957	-3.03

SLC16A9	0.001067267	2.81
SLC18A3	1.13E-05	-6.00
SLC1A6	0.008064911	-3.68
SLC22A23	0.026642657	-2.13
SLC25A22	0.082649104	-2.10
SLC25A24	5.01E-05	3.58
SLC25A27	0.051973595	-2.70
SLC26A10	0.055207882	-2.59
SLC26A2	0.038621339	1.82
SLC29A1	0.000272462	2.86
SLC2A4RG	0.048152774	1.81
SLC32A1	6.52E-05	-2.65
SLC35F1	7.50E-05	-3.10
SLC40A1	0.08680324	1.76
SLC43A2	0.01076115	-2.83
SLC44A1	0.062582189	1.87
SLC45A4	0.017041785	2.45
SLC4A8	0.001773233	-3.03
SLC6A1	0.092305481	-1.76
SLC6A13	0.009781286	14.63
SLC6A3	0.010226599	5.83
SLC6A7	7.59E-05	-30.00
SLC7A7	0.00189433	4.13
SLC8A2	0.001497451	-2.63
SLC9A9	0.040262621	1.89
SLFN11	0.017494596	2.41
SLFN5	0.058168121	2.29
SMARCD2	0.075159057	1.74
SMC6	0.088996687	1.80
SMOC2	5.06E-06	3.45
SMPD3	3.63E-11	-5.61
SMTNL2	0.006887367	3.91
SNAI1	0.000269519	4.42
SNAI2	6.39E-06	3.50
SNHG5	7.36E-06	3.65
SNHG8	0.021798893	2.08

SNORD116-12	0.098454251	416.25
SNX10	0.000100096	-3.57
SOCS7	0.075594096	-2.43
SOGA3	5.17E-07	-3.98
SORBS2	0.007973845	-2.33
SORL1	0.00084042	-2.97
SOX1	0.00824458	-2.20
SOX11	0.000715888	-3.16
SOX2-OT	0.000680764	-3.00
SOX4	0.001680751	-3.57
SPAG4	0.065867426	-3.96
SPATA13	0.000625419	-2.95
SPG21	0.060448256	1.73
SPIDR	0.07614192	1.67
SPIRE2	0.027631254	-2.82
SPNS2	0.048462151	-2.52
SPON1	0.02071709	2.51
SPP1	0.011828489	-2.87
SPRR3	0.007606414	-101.33
SPTBN2	0.00179205	-2.61
SRCIN1	4.34E-05	-3.20
SRGAP3	0.010575763	-2.12
SRRM3	0.051215703	-2.14
SRRM4	0.036036065	-2.12
SSFA2	0.096499705	-1.98
SSPN	0.001773233	2.43
ST3GAL6	0.061428385	-3.76
ST8SIA1	0.002121041	-2.69
ST8SIA2	2.97E-06	-3.73
STAG3	0.048544065	-2.52
STARD13	0.087729326	1.82
STAT6	0.01306124	2.09
STEAP3	0.050998297	1.59
STK38	0.044803646	1.86
STK38L	0.055408467	1.91

Nature Neuroscience: doi:10.1038/nn.4532

STMN3	0.047122136	-2.18
STOX2	0.001339306	-2.88
STRBP	0.080288916	-1.93
STX12	0.053192545	-2.14
SULF2	0.011111988	3.17
SVIP	0.053291335	-2.66
SVOP	2.25E-10	-7.60
SYN2	0.056730949	2.30
SYNDIG1L	5.94E-05	-8.27
SYNJ1	0.04374308	-1.98
SYNJ2	0.026675778	2.21
SYT11	0.007438721	-2.68
SYT13	1.78E-13	-5.52
SYT16	0.030677372	-3.51
TAC3	3.20E-11	-15.12
TAGLN3	0.048110458	-2.28
TARBP1	0.04981449	-2.28
TBC1D2B	0.02687182	2.16
TBX1	0.000463481	8.19
TBX15	2.83E-14	7.78
TBX3	0.029247104	2.74
TCEA3	0.002309656	5.23
TCF15	0.00576802	-8.15
TCTA	0.089937933	1.85
TCTE1	0.083130546	-3.63
TEAD4	1.10E-06	9.26
TEF	0.007492346	2.31
TENC1	0.035888481	1.84
TET1	0.011799165	-1.97
TFF2	0.012846946	-101.33
TFR2	0.000135498	-8.28
TGFBR2	7.84E-06	3.52
TGFBR3	3.59E-09	4.63
THBD	0.001836309	4.33
THBS3	0.01586154	2.05
THY1	0.026467147	1.97
TIGD3	0.048219253	-4.03
TJP3	0.010547743	-3.71
TLE4	0.08338071	-1.94
TLN1	0.084935884	1.72
TMC4	0.041365909	-6.02
TMEFF1	5.70E-05	-3.22
TMEM109	7.22E-05	3.08
TMEM119	1.86E-09	5.51
TMEM130	0.0195434	-2.60
TMEM145	4.13E-05	-4.50
TMEM178A	0.002115216	-2.92
TMEM182	0.033010125	2.21
TMEM189	0.014044073	2.04
TMEM196	0.000263506	-3.75
TMEM214	0.033280648	1.87
TMEM26	0.022871713	2.66
TMEM260	0.076397906	1.80
TMEM38B	0.000188967	3.45
TMEM56	0.000635936	2.79
TMEM64	0.006025875	2.35
TMEM74	0.016950125	-3.84
TMEM74B	0.000142451	-3.68
TNFRSF11B	0.010629284	3.14
TNFRSF1A	0.067246363	1.59
TNFSF13B	0.009525841	14.60
TNFSF4	0.033804754	3.20
TNNI3	0.005922035	-6.24
TNPO2	0.082801034	-2.11
TOX2	1.54E-05	-3.67
TPM1	2.84E-12	6.57
TPPP3	0.065322419	2.13
TRH	1.67E-09	-6.20
TRIB1	0.000317038	-3.72
TRIB2	0.002839924	-2.79
TRIL	0.003843542	2.33
TRIM24	0.018901298	-2.15
TRIM38	0.002806819	4.86
TRIM54	0.000342575	9.60
TRIM62	0.008627726	2.36
TRIM63	6.64E-11	14.60
TRIM71	0.012036057	-5.90
TRPC6	6.65E-10	27.35
TRPV4	0.009176826	5.83
TSHZ3	0.038498303	1.96
TSKU	0.013985553	2.01
TSPAN13	0.002058546	-2.65
TSPAN2	0.087076367	-2.31
TTBK1	4.72E-09	-5.36
TTC9B	4.57E-08	-6.14
TTYH2	0.067212371	1.69
TUB	0.040168991	-2.20
TUBB2A	0.003025684	-2.72
TUBB2B	2.61E-05	-3.90
TUBB3	9.10E-05	-3.91
TUBB4A	3.59E-08	-4.16
TWIST1	0.00837844	2.98
TXNDC5	0.00795843	2.30
UBE2E3	0.098592244	1.66
UBL3	0.017522233	-2.30
UGT3A1	0.063314511	7.14
UGT3A2	0.058175675	5.51
ULBP2	0.046661428	-4.25
UNC79	0.000159797	-3.59
USH1G	0.018745352	-4.22
USO1	0.056348437	1.84
USP49	0.077845086	-2.49
UTS2B	0.006377201	13.01
UXS1	0.065050619	1.65
VANGL2	0.037726825	-2.11
VCAN	0.010258307	3.00
VDR	0.003832813	4.36
VEGFA	0.000205201	-3.69

Nature Neuroscience: doi:10.1038/nn.4532

VGLL3	1.79E-11	7.07
VILL	0.012011559	-8.36
VIP	0.087121163	-7.86
VIPR1	0.036900937	-9.47
VSTM4	0.031398118	3.94
VSX2	0.014965805	-2.64
VTCN1	0.00490984	-7.13
WARS	0.058758705	1.82
WDR47	0.004670586	-2.45
WDR54	0.072125703	-2.54
WHSC1	0.095041048	-1.88
WIF1	0.00041246	3.08
WISP2	0.05362389	6.75
WNT10B	0.007677907	-4.46
WNT11	1.84E-05	4.73
WNT6	0.00968876	7.18
WRNIP1	0.08947526	1.64
WSB1	0.040393581	-2.41
WWC1	0.001455538	-2.67
XIRP1	0.000156131	21.63
XKR7	2.72E-08	-12.87
YBX2	0.071110448	-2.78
YBX3	5.51E-06	3.83
YWHAH	0.058168121	-2.15
ZBBX	0.089640893	-4.36
ZBTB16	0.01697557	-3.27
ZC3H6	0.051769753	-2.09
ZDHHC22	0.018815629	-2.54
ZDHHC5	0.044492011	1.79
ZFR2	0.011887328	-3.78
ZMIZ1	0.088259931	-2.08
ZNF106	2.11E-05	4.54
ZNF25	0.053260605	-2.01
ZNF469	0.009305985	2.73
ZNF471	0.003057712	3.90
ZNF502	0.031229521	4.11
ZNF532	0.067128265	-2.01
ZNF540	0.030398891	-2.85
ZNF697	0.087076367	-1.98
ZNF702P	0.098543092	-2.06
ZNF804A	0.004954068	-4.52
ZNF835	0.077899659	9.78
ZPLD1	0.076060133	-4.02

Table S2: RNA-Seq DEGs and highlighted mouse striatal development genes.

1869 genes, excluding X- and Y-linked genes, were differentially expressed by RNA-Seq analysis, with FDR (False discovery rate) adjusted p-value cutoff set to 10%. Fold-change was calculated and displayed as HD/non-disease. 679 common genes found to be involved in mouse striatal development have been highlighted in red.

Nature Neuroscience: doi:10.1038/nn.4532

Gene Symbol	Adjusted p-value	Fold Change
TGFBR3	3.59E-09	4.63
HES5	8.27E-02	-3.19
GAD2	1.10E-02	-2.83
ASCL1	2.99E-02	-2.11
TGFB3	2.40E-06	3.74
DLL3	8.44E-04	-4.03
NEUROD1	1.40E-16	-14.20
GAD1	2.68E-09	-5.53
SLC32A1	6.52E-05	-2.65
ADORA2A	4.73E-03	-3.74
TGFBR2	7.84E-06	3.52
NEUROG2	3.47E-09	-17.37
POU4F2	4.30E-09	-19.11
HEY2	1.41E-02	2.78
RREB1	2.06E-02	2.14
CREB5	5.07E-02	-1.88

Table S3. Genes from Figure 2b

Fold Change and adjusted p-values for genes from Figure 2b.

Upstream Regulator	Fold Change	Predicted Activation State	Activation z-score	p-value of overlap
REST		Activated	4.038	3.63E-14
KDM5B		Activated	3.449	1.08E-01
HTT		Activated	3.288	4.07E-18
TGFB1		Activated	3.088	1.68E-23
IL1B		Activated	2.543	2.54E-13
MYOD1		Activated	2.380	4.51E-08
TGFBR1		Activated	2.173	5.22E-03
IL13		Activated	2.089	1.65E-05
BMP2	2.717	Activated	2.014	5.49E-07
NCOA2		Activated	2.000	3.12E-01
NEUROD1	-14.200		-1.985	3.51E-04
BDNF		Inhibited	-2.089	6.98E-15
ASCL1	-2.114	Inhibited	-2.574	4.01E-06
ADORA2A	-3.744	Inhibited	-2.721	4.17E-07
NRG (family)		Inhibited	-2.828	1.42E-04
miR-124-3p		Inhibited	-3.638	3.05E-06

Table S4. Predicted upstream regulators from RNAseq

Upstream analysis of RNA-Seq DEGs. Genes with a |z-score| > or < 2.0 are assigned a predicted activation state, allowing inferred protein activity based on observed differential gene expression. Analysis of HD DEGs predicts activation or inhibition of several genes known to be involved in HD pathogenesis, as well as possible novel regulators.

a

Class 1 genes GO term	FDR
skeletal system development	5.06E-27
neuron differentiation	8.73E-31
transcription factor activity	3.24E-25
extracellular region part	2.72E-16
regulation of transcription from RNA pol	9.98E-19
regulation of cell development	6.66E-15
signal	9.45E-16
vasculature development	1.02E-10

b

Class 1 genes GO term	FDR
nucleus	3.46E-56
regulation of transcription from RNA pol	1.39E-44
sequence-specific DNA binding	7.38E-42
pattern specification process	1.02E-21
neuron differentiation	2.20E-24
embryonic morphogenesis	4.23E-22
isopeptide bond	1.25E-19
nuclear lumen	1.07E-15
transcription factor binding	6.20E-14

c

Class 5 genes GO term	FDR
synapse	7.09E-08
synaptic transmission	2.71E-06
ligand-gated ion channel activity	6.39E-04
ionic channel	1.82E-07
extracellular matrix	2.13E-02
membrane	2.96E-04
glutamate receptor activity	7.96E-03
ion binding	9.90E-05
cell projection organization	3.74E-02
neurotransmitter transport	2.54E-03

d

HD-enriched genes GO term	FDR	Control-enriched genes GO term	FDR
cadherin N-terminal	1.40E-21	plasma membrane part	5.28E-08
muscle system process	2.11E-08	signal	2.53E-09
contractile fiber	1.55E-13	domain:fibronectin type-III 2	1.04E-05
signal	2.07E-09	plasma membrane	3.83E-08
calcium-dependent cell-cell adhesion	6.68E-05	Immunoglobulin subtype 2	2.37E-03
proteinaceous extracellular matrix	3.53E-04	sequence-specific DNA binding	2.68E-02
synaptic transmission	4.33E-04	ion transport	8.86E-04
repeat:PXXP	1.67E-02		
glycoprotein	4.52E-09		
muscle organ development	4.60E-12		

e

HD-enriched genes GO term	FDR	Control-enriched genes GO term	FDR
myofibril	4.14E-09	synaptic transmission	1.39E-11
muscle contraction	1.01E-06	neuron differentiation	4.69E-09
actin cytoskeleton	7.72E-05	topological domain:Cytoplasmic	4.32E-06
muscle organ development	3.37E-06	plasma membrane part	1.67E-06
muscle protein	2.39E-02	glycoprotein	1.99E-05
cytoskeleton	8.30E-03	ionic channel	8.79E-07
dystrophin-associated glycoprotein complex	7.20E-03	hsa04080:Neuroactive ligand-receptor interaction	6.98E-05
striated muscle tissue development	1.14E-02	adult behavior	3.30E-03
		neuron projection	1.25E-04
		chemical homeostasis	1.53E-02

Table S5. GO term enrichment of Class 1 genes, H3K36me3 enriched genes, H3K4me3 enriched genes, and and genes with differential H3K27Ac peaks.

(a) & (b) GO terms assigned to genes falling under the Class 1 epigenetic profile for H3K27Ac and H3K4me3, respectively. (c) GO terms assigned to genes falling under the Class 5 epigenetic profile for H3K36me3. (d) GO terms assigned to genes with higher H3K4me3 peaks in HD or non -disease cells, respectively. GO terms and false discovery rate adjusted p values were found using DAVID Functional Annotation Clustering tool. The top GO term from each annotation cluster is reported. (e) Enriched (increased acetylation/peak height) genes in HD show categories related to muscle development, function, and cytoskeleton; while non-disease-enriched genes show categories related to neuronal development and function.

Supplementary Note: Consortium Groups

Departments of Biological Chemistry, Psychiatry and Human Behavior, Neurobiology and Behavior, UCI MIND and Sue and Bill Gross Stem Cell Center, University of California, Irvine, Irvine, California USA.
Ryan G. Lim, Lisa. L. Salazar, Alvin R. King, Jennifer T. Stocksdale, Delaram Sharifabad, Alice L. Lau, Jack C. Reidling, Sara T. Winokur, Malcolm S. Casale, Leslie M. Thompson

Department of Biomedical Sciences, Faculty of Medicine and Health Sciences, University of Barcelona, Barcelona; August Pi i Sunyer Biomedical Research Institute (IDIBAPS), Casanova 143, 08036 Barcelona, Spain and Networked Biomedical Research Centre for NeuroDegenerative Disorders (CIBERNED), Spain.
Mónica Pardo, A. Gerardo García Díaz-Barriga, Marco Straccia, Phil Sanders, Jordi Alberch, Josep M. Canals

Gladstone Institutes and the Taube/Koret Center of Neurodegenerative Disease Research, Roddenberry Stem Cell Research Program, Departments of Neurology and Physiology, University of California, and Cliff Anderson-Bergman Sandia National Laboratories, 7011 East Avenue, Livermore, California USA.
Julia A. Kaye, Mariah Dunlap, Lisa Jo, Hanna May, Elliot Mount, Kelly Haston, Steven Finkbeiner

Computational and Systems Biology Graduate Program, Massachusetts Institute of Technology, Center for Cancer Research, Department of Biological Engineering and/or Department of Biology, Massachusetts Institute of Technology, Cambridge, Massachusetts USA.
Amanda J. Kedaigle, Theresa A. Gipson, Ferah Yildirim, Christopher W. Ng, Pamela Milani, David E. Housman, Ernest Fraenkel

School of Biomedical Sciences, Sir Martin Evans Building, Museum Avenue, Cardiff University, Cardiff, CF10 3AX, UK
Nicholas D. Allen, Paul J. Kemp

Center for Human Genetic Research, Simches Research Building, 185 Cambridge Street, Massachusetts General Hospital, Boston, Massachusetts USA.
Ranjit Singh Atwal, Marta Biagioli, James F. Gusella, Marcy E. MacDonald

Division of Neurobiology, Department of Psychiatry, Departments of Neurology, Neuroscience and Pharmacology and Program in Cellular and Molecular Medicine, Johns Hopkins University School of Medicine, Baltimore, Maryland USA.
Sergey S. Akimov, Nicolas Arbez, Jacqueline Stewart, Christopher A. Ross

F.M Kirby Neurobiology Center, Boston Children's Hospital, Harvard Medical School (HMS), Boston, Massachusetts USA.
Daniel K. Wilton, Beth Stevens

The Board of Governors Regenerative Medicine Institute and Department of Biomedical Sciences; Cedars-Sinai Medical Center; Los Angeles, California USA.
Virginia B. Mattis, Colton M. Tom, Loren Ornelas, Anais Sahabian, Lindsay Lenaeus, Berhan Mandefro, Dhruv Sareen, Clive N. Svendsen